Fate of NO and Ammonia in Chemical Looping Combustion-Investigation in a 300 W Chemical Looping Combustion Reactor System

N.B. When citing this work, cite the original published paper.

(article starts on next page)

Fate of NO and Ammonia in Chemical Looping Combustion—Investigation in a 300 W Chemical Looping Combustion Reactor System

Anders Lyngfelt,* Ali Hedayati, and Ellen Augustsson

ACCESS | Metrics & More | Article Recommendations

ABSTRACT: Chemical looping combustion (CLC) is a novel combustion concept that transfers oxygen from air to fuel using an oxygen carrier that circulates between an air reactor and a fuel reactor. Thus, the combustion products, H_2O and CO_2, are obtained in a separate flow, and ideally, a pure CO_2 gas stream is obtained after condensation of H_2O. Consequently, CLC has a unique potential for avoiding the high costs and energy penalties of CO_2 capture. Further, NO emissions can potentially be avoided. CLC is flameless, and the temperature is too low for the formation of thermal NO_x. Moreover, fuel NO_x and prompt NO_x do not form in the air reactor in the absence of fuel. In the fuel reactor, the absence of oxygen prevents normal NO_x formation. However, when using fuels containing nitrogen, NO may form in the fuel reactor

because the oxygen carrier can oxidize fuel nitrogen compounds. To achieve a CO_2 stream suited for storage, NO must be removed. Dependent upon how NO is removed, the process could be free from any NO emissions. NO formation and NO reduction were investigated in a 300 W CLC reactor by adding either NH_3 or NO. The work involved two different oxygen carriers, Linz−Donawitz (LD) slag and ilmenite, two temperatures, 850 and 900°C, two circulation rates, and different flows of syngas fuel. Further, operation without fuel with a fully and partially oxidized oxygen carrier was studied. For LD slag, lower fuel flow promoted the formation of NO and decreased the reduction of NO. Likewise, higher temperatures raised NO formation and lowered NO reduction. Ilmenite, however, was by far more superior with respect to NO. Thus, NO formation only occurred in the absence of fuel and with a fully oxidized oxygen carrier. Likewise, NO was fully reduced to N_2 for all conditions, except in the absence of fuel and with fully oxidized ilmenite.

1. INTRODUCTION

One approach to reduce CO_2 emissions is to implement carbon capture and storage (CCS), whose purpose is to
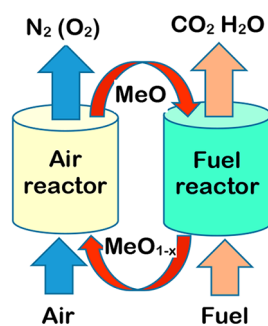
Figure 1. CLC principle. MeO is the metal oxide circulated. This figure was reproduced with permission from ref 1. Copyright 2020 American Chemical Society.

capture CO_2 emissions and store them. The conventional methods of carbon capture are however highly energy-intensive processes and require a larger fuel input to sustain the increased energy demand. To achieve so-called negative CO_2 emissions, CCS can be conducted in combination with carbon-neutral fuels, i.e., biomass or waste streams of biogenic origin. This is called bioenergy with carbon capture and storage (BECCS).

1.1. Chemical Looping Combustion (CLC). CLC is a novel combustion technology that can be used for the purpose of CO_2 capture, without the large energy penalty of conventional capturing methods. It consists of two inter-
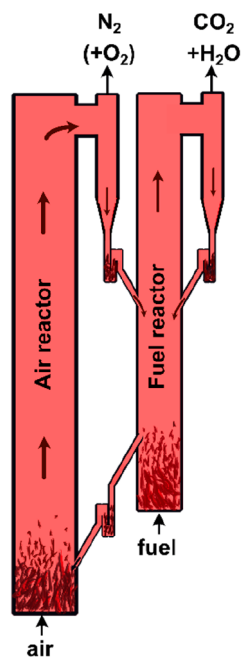
Figure 2. CFB reactor system for gas. This figure was reproduced with permission from ref 2. Copyright 2022 American Chemical Society.

connected fluidized bed reactors, an air reactor and a fuel reactor, where the oxygen carrier is cycled between the reactors (Figure 1). A typical reactor system with interconnected fluidized beds is shown in Figure 2.

In the air reactor, the oxygen carrier will be oxidized and the oxidation of a generic oxygen carrier with oxygen provided from the air can be represented by
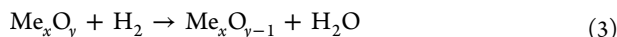
$$2Me_xO_{y-1} + O_2 \rightarrow 2Me_xO_y \tag{1}$$
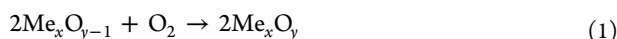
The gas stream out of the air reactor consists of N_2 and some remaining oxygen. The reaction in the air reactor, eq 1, is always exothermic. In the fuel reactor, the oxygen carrier will be reduced by the fuel.

The following two equations describe the reduction of a generic oxygen carrier with syngas:

$$Me_xO_y + CO \rightarrow Me_xO_{y-1} + CO_2 \tag{2}$$

and

$$Me_xO_y + H_2 \rightarrow Me_xO_{y-1} + H_2O \tag{3}$$
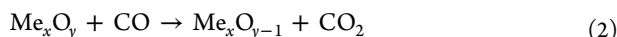
The flue gases from the fuel reactor consist of mainly CO_2 and steam, where the steam can easily be condensed to create a CO_2-rich stream. The reactions in the fuel reactor can be either endothermic or exothermic, depending upon the combination of the oxygen carrier and fuel. The net energy release in the CLC unit is the same as in conventional combustion.

1.2. Oxygen Carrier. The oxygen carrier is crucial in CLC and needs to perform its duty of transferring oxygen, without being rapidly mechanically or chemically degraded. The number of materials examined in laboratory are of the order of a thousand, whereas the number of materials examined in pilot operation are in the order of a hundred. Oxygen carrier materials investigated in pilot operation include manufactured monometallic oxide systems, i.e., oxides of Ni, Fe, Mn, Cu, and Co, normally using an inert support as well as several combined oxide systems, primarily combined Mn oxides. Moreover, many low-cost natural ores and waste materials have

been examined, including ilmenite, manganese, and iron ores. Total pilot operation includes 12 000 h in 49 CLC pilots of sizes up to 3 MW, presented in more than 200 publications.[1,3−8] Normally but dependent upon the oxygen carrier, the gas coming from the fuel reactor is not fully oxidized to CO_2 and H_2O. Therefore, an oxy-polishing step may be required, where any remaining combustibles are burnt by oxygen added.

1.3. Chemical Looping with Oxygen Uncoupling (CLOU). A variant of CLC is CLOU. In CLOU, the oxygen carrier spontaneously releases molecular oxygen to the gas phase instead of being reduced by the fuel.[9] Thus, the reduction of the oxygen carrier in CLOU can be expressed as

$$2Me_xO_y \rightarrow 2Me_xO_{y-1} + O_2 \tag{4}$$
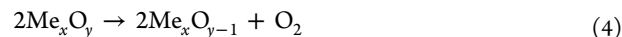
whereas the oxidation of the oxygen carrier is similar to normal CLC. To work, the oxygen carrier needs to have an equilibrium partial pressure that is below the oxygen concentration in the air reactor and above the oxygen concentration in the fuel reactor, which is close to zero as oxygen is consumed by the fuel. Thus, a suitable CLOU material can have an equilibrium partial pressure corresponding to around 1−3% oxygen. Thus, the fuel burns in oxygen being released.

Potential oxygen carriers for CLOU are based on copper[9−11] and combined manganese oxides.[12] The latter includes manganese oxides combined with iron, nickel, silicon, calcium, and magnesium[12−18] as well as ternary systems.[19] Copper oxide is the most potent CLOU material, and full gas conversion has been reported from pilot operation.[20,21] For combined mangese materials, best results thus far were obtained with calcium manganite, $CaMnO_3$, a perovskite with oxygen-releasing properties. More than 700 h of operation with calcium manganates in seven different pilots of 0.3−1000 kW, mostly with gaseous fuels, clearly demonstrates that these materials show high performance, long lifetime, and, under good conditions, even full gas conversion.[22−36]

2. NITROGEN OXIDES

Nitrogen oxides (NO_x) include nitric oxide (NO), nitrogen dioxide (NO_2), and nitrous oxide (N_2O). NO is the main NO_x
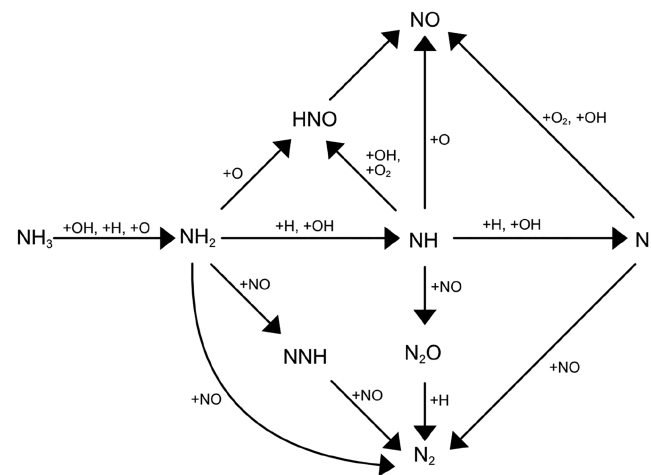

Figure 3. Reaction paths for the oxidation of NH_3 in combustion processes according to Miller and Bowman.[43] This figure was reproduced with permission from ref 43. Copyright 1989 Elsevier.

Table 1. Nitrogen Species in the Bottom of a 12 MW Circulating Fluidized Bed Boiler[44]

	bottom (ppm)	flue gas (ppm)
nitric oxide, NO	520	55
ammonia, NH_3	1090	
hydrogen cyanide, HCN	240	
isocyanic acid, HNCO	250	
nitrous oxide, N_2O	15	140
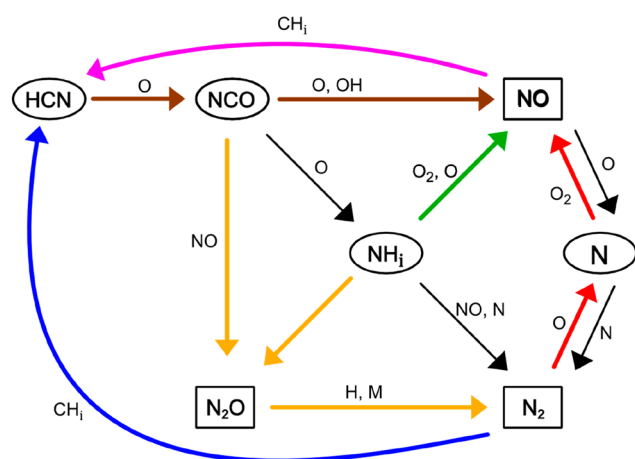
Figure 4. Overview of important reactions in nitrogen chemistry starting from compounds such as HCN or NH_i: red, thermal NO_x; blue, prompt NO_x; brown, fuel NO_x coal; green, fuel NO_x biomass; yellow, N_2O formation/reduction; and cyan, reburning.

product formed during combustion. In normal combustion processes, there are three distinct paths of NO_x formation: thermal NO_x, prompt NO_x, and fuel NO_x, which are further described below.

2.1. Thermal NO_x. Thermal NO_x is created when molecular oxygen and molecular nitrogen react at high temperatures, according to the Zeldovich mechanism.

$$N_2 + O \rightarrow NO + N \tag{5}$$

$$N + O_2 \rightarrow NO + O \tag{6}$$

$$N + OH \rightarrow NO + H \tag{7}$$

The formation of thermal NO_x is only significant at high temperatures, above 1500°C.[37] In combustion, local high temperatures are associated with flames. In combustion with no fuel-bound nitrogen, thermal NO_x is responsible for most of the NO_x emissions produced.

In CLC, flames are absent and the temperature in both the air and fuel reactors is far below that needed for thermal NO_x formation. In the fuel reactor, the absence of oxygen and the minute presence of N_2 would also prevent thermal NO_x formation. Thus, thermal NO_x formation can be excluded in CLC, except possibly for the oxy-polishing step, downstream of the fuel reactor.

2.2. Prompt NO_x. In fuel-rich environments, hydrocarbon radicals, such as C and CH, are formed that can react with molecular nitrogen to produce carbon-containing nitrogen species[38]

$$C + N_2 \rightarrow CN + N \tag{8}$$

and

$$CH + N_2 \rightarrow HCN + N \tag{9}$$

NO_x is subsequently formed by oxidation of these nitrogen compounds. This mechanism is referred to as prompt NO_x.[39] Prompt NO_x only contributes to a small fraction of the total NO_x emissions.[39] In the air reactor, the formation of prompt NO_x is not possible in the absence of volatile organic compounds. In the fuel reactor, N_2 is only present in minute amounts, and therefore, it would be highly unlikely that prompt NO_x formation is significant in CLC.

2.3. Fuel NO_x. Nitrogen is found in almost all solid fuels, is bound to the fuel structure, and can be released both from the char conversion as well as in the form of volatile matter released during pyrolysis.[37] The temperature, the heating rate, and the fuel structure affect how nitrogen is divided between the volatile matter and the char.[37] The nitrogen species that are present within the volatiles are mainly hydrogen cyanide (HCN) and ammonia (NH_3).[40] For high-rank fuels, such as coal, HCN is considered to be the main nitrogen species released during pyrolysis, whereas for low-rank fuels, such as biomass, NH_3 stands for the majority of nitrogen species in the volatiles.[41] In addition to the fuel type, the heating rate, and the final temperature, the residence time also affects the distribution of the nitrogen species released during pyrolysis.[40]

The intermediate nitrogen species formed during combustion (HCN, NH_3, etc.) can both react with oxygen species to create NO and with NO produced to form N_2.[42] For NH_3, the general reaction involves oxidation of NH_3 to NH_i radicals (i = 0, 1, and 2), where the radicals can be further oxidized to produce NO or react with NO to form N_2 (cf. Figure 3).[43]

In situ gas measurements in the bottom of a 12 MW circulating fluidized bed boiler fired with bituminous coal are shown in Table 1.[44] The concentrations measured indicate that the bottom zone is highly reducing, which is because there is a large bypass of the fluidizing air. The high velocity of the bypassing gas means that this flow is underrepresented in the gas measurement, which is made by a suction probe that is most of the time in the dense phase, where the fuel releases volatiles and the char removes oxygen.[45] Thus, the gas concentrations measured do not represent the gas flow. On the basis of measured total carbon of around 21%, the concentrations in Table 1 can be normalized to 15% CO_2 by division by 1.4.

Even with normalization, the data in Table 1 indicate high concentrations of NO as well as other precursors discussed above. The comparison to the flue gas shows that the NO concentration falls dramatically, whereas N_2O rises. It can also be noted that there are several potential NO precursors present in high concentrations.

2.4. Nitrous Oxide, N_2O. N_2O emissions have been found to be of importance in fluidized bed combustion but of minor importance in other combustion systems,[37] which is explained by the low temperature in fluidized bed combustion.[46] Thus, an increase in the temperature from normal operating temperature at 850 to 925°C decreased N_2O by a factor of 3 at 2% O_2. The results presented here for N_2O come from work in a 12 MW circulating fluidized bed boiler. It was also found that N_2O could be decreased by more than 90% by afterburning, i.e., adding fuel that raises the cyclone temperature to 950°C.[46] Five different fuels were added, and the decrease in N_2O versus the cyclone temperature in the range of 850−950°C was identical for these. With so-called reversed air staging, it was possible to reduce N_2O emissions from 60 ppm

to just a few parts per million at 970°C.[47] The method involved keeping the riser at slightly overstoichiometric conditions and then adding air after the cyclone outlet. Moreover, experiments with injection of N_2O in the bottom of the riser found that 80−97% of N_2O was reduced.[44]

Further, there seems to be essentially no formation of N_2O when burning high-volatile fuels. Thus, at 950°C, 130−140 ppm of N_2O was found in the flue gas for bituminous coal and coke, whereas for wood chips, 0−10 ppm was found.[48]

With the high fuel reactor temperatures typical for CLC, e.g., >950°C, and the absence of oxygen, it can be expected that no N_2O will form, i.e., unless it is formed from reactions with the oxygen carrier.

2.5. Reburning. At understoichometric conditions, NO can be reduced. Introduction of fuel immediately after the main combustion stage to create a fuel-rich zone can be used to reduce NO to HCN. The process is called reburning.

2.6. Summary. The important reactions for the nitrogen chemistry in combustion are summarized in Figure 4. The scheme is simplified and does not consider all potential or existing reaction paths. It includes the main precursors formed when fuels are devolatilized, HCN and NH_3. However, in addition to the gas-phase reactions outlined, various nitrogen compounds are also formed during the char combustion, including N_2, N_2O, NO, HCN, and NH_3.[40]

As indicated above, there is good reason to assume that neither thermal NO_x nor prompt NO_x formation takes place in CLC. Moreover, the formation of N_2O is not likely, and in any way, a reduction of N_2O should be efficient at the high temperature and slightly understoichiometric conditions of a fuel reactor. In the case of fuel NO_x, the main reactions leading to NO are obviously promoted by the presence of oxygen, which is absent in the fuel reactor. Moreover, the formation of oxidized nitrogen compounds during char conversion, i.e., gasification, is less likely in the absence of oxygen. At the slightly understoichiometric conditions of the fuel reactor, reburning of NO could be possible, depending upon the presence of radicals. As seen in Figures 3 and 4, the gas phase reactions involve a number of radicals, i.e., O, OH, H, N, and CH_i. However, there are two reasons to assume that radical concentrations are lower in fluidized beds: first, the temperature is lower than in normal flame combustion, and second, radicals may be quenched by the surface of the bed material. Johnsson[40] investigated NO_x formation and reduction in fluidized bed combustion (FBC) and concluded that it is unknown how the high solid concentration will affect the radical chemistry. Löffler et al.[49] developed a mechanism describing NO_x formation in a fluidized bed (FB), in which they proposed that the high solid concentration is causing radical quenching. The mechanism included the radical recombination reactions of O, H, OH, and HO_2 that occur on the surfaces of the solid bed material. Radical quenching is also included in the work of Kilpinen et al.,[50] where NO_x formation and reduction are modeled in FBC.

3. EQUILIBRIUM CONCENTRATIONS

In the absence of oxygen or under the more or less reducing conditions in a fuel reactor, any nitrogen species, i.e., except for N_2, is below or well below 1 ppm, as shown in Figure 5. Here, the gas is a 50:50 mixture of steam and CO_2 with 1% N_2, and the temperature is 950°C. Oxygen is stepwise-removed from the system, which gradually increases the gas content of CO and H_2. NO dominates at stoichiometry, whereas NH_3
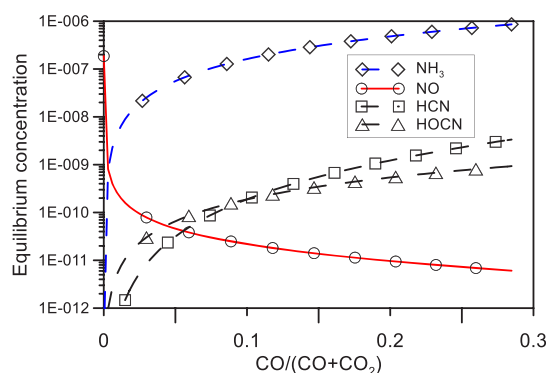

Figure 5. Equilibrium composition of nitrogen species under conditions in a fuel reactor.

becomes dominant as soon as the $CO/(CO + CO_2)$ ratio becomes higher than 0.005. Equilibrium calculations were made with HSC Chemistry 5.11 for Windows.[51] The conditions in the experiments presented in this paper all have a $CO/(CO + CO_2)$ ratio within the range of 0−0.1, which means that any measurable amounts of NO or NH_3 represent a deviation from equilibrium.

4. CLC RESEARCH RELATED TO NO

NO_x formation in CLC applications has been investigated experimentally, in both laboratory-scale fluidized bed reactors and connection with operation of 0.5−100 kW CLC units.

4.1. Batch Reactor Experiments. Ishida and Jin[52] were the first to study NO_x formation in CLC and found that no NO is found when oxidizing a nickel-based oxygen carrier at 1200°C.

Cheng et al.[53] investigated the possible reactions between NH_3 and ilmenite in a laboratory-scale fluidized bed reactor, in the presence of syngas. They found that around 18% of NH_3 was converted to NO independent of the temperature in the investigated range, 850−950°C. The remainder was converted to N_2, except at 850°C, where small amounts of unconverted NH_3 were seen. When the NH_3 inlet concentration was lowered from 1 to 0.2%, there was a strong increase in the fraction of NO and a corresponding decrease in N_2. Not unexpected, the conversion to NO fell with the increasing syngas concentration in the range of 0−40%. However, even at the highest syngas concentrations, NO was formed. Also, the ability of ilmenite to reduce NO was studied as a function of the degree of oxidation and in the absence of fuel. Fully oxidized ilmenite did not reduce NO, and the reduction of NO was almost linear to the conversion of ilmenite.

Normann et al.[54] studied the oxidation of NH_3 for three different oxygen carriers based on oxides of Fe, Mn, and Ni in a laboratory-scale fluidized bed reactor. The oxygen carrier was alternatingly exposed to syngas and 1% NH_3, with periods of inert gas in between. Thus, the oxidation of NH_3 could be examined as a function of the degree of conversion of the oxygen carriers. For NiO, no NO was formed independent of the oxidation level of the oxygen carrier. For iron oxide, the conversion to NO was initially around 40%, i.e., for fully oxidized iron oxide, and gradually decreased to zero as the oxygen carrier became fully reduced. For manganese oxide, on the other hand, the conversion was well above 60% for most of the conversion and only dropped to zero in the last part of the reduction.

Table 2. Nitrogen Compounds Measured in Operation of CLC Pilots

reference	size (kW)	oxygen carrier	temperature (°C)	fuel	inlet N fraction	NO_x (ppm, normalized)	N conversion to NO_x (%)
Song et al.[57]	1	NiO	850−950	bituminous coal	1.03% ad[b]	400−630	
Song et al.[57]	1	NiO	850−950	anthracite	1.39% ad[b]	1−20	
Song et al.[58]	1	Fe_2O_3	970	bituminous coal	1.03% ad[b]	0	0
Song et al.[58]	1	Fe_2O_3	970	anthracite	1.39% ad[b]	0	0
Markström et al.[59]	100	ilmenite	960	bituminous coal	1.65% daf[a]	1000−2000	10−20
Linderholm et al.[60]	100	ilmenite	950−970	wood char	0.4% daf[a]	500 (850)	7−32
Linderholm et al.[60]	100	ilmenite	960	petcoke	1% daf[a]		3−8/20
Linderholm et al.[61]	100	ilmenite	970	bituminous coal	1.6% daf[a]		11 of gas/5.6 of total
Linderholm et al.[62]	100	ilmenite + manganese ore	963−971	bituminous coal	1.6% daf[a]		29 of gas
Linderholm et al.[63]	100	iron ore	895−950	bituminous coal	1.6% daf[a]		10 of gas
Linderholm et al.[64]	100	manganese ore	950−979	bituminous coal	1.6% daf[a]		4−11 of gas
Mendiara et al.[65]	0.5	ilmenite	875/930	lignite	0.6%	20	1
Mendiara et al.[66]	0.5	iron ore		pine sawdust	0.28%		4−14
Mendiara et al.[66]	0.5	iron ore		olive stone	0.18%		4−14
Mendiara et al.[66]	0.5	iron ore		almond shell	0.16%		4−14
Gu et al.[67]	1	Fe_2O_3	880−980	bituminous coal	1.03% ad[b]	24−68	0.5−0.8
Bayham et al.[68]	25	Fe_2O_3	970	sub-bituminous coal		1148−1669	10−15
Ohlemüller et al.[69]	1000	ilmenite and iron ore		coal and coal + biomass	1.81 and 0.17%	0, 20, and 8	

[a]daf = dry and ash-free. [b]ad = air dried.

Normann et al.[55] investigated the oxidation of NH_3 using an oxygen carrier with CLOU properties, copper oxide. The experiments were conducted in a laboratory-scale fluidized bed reactor with syngas as fuel, and the inlet fractions of NH_3 and syngas were varied. They concluded that the nitrogen selectivity is highly dependent upon the oxidation level of the oxygen carrier; a higher oxidation level promotes the nitrogen selectivity toward NO. They also found that the nitrogen selectivity is affected by syngas; a higher concentration of syngas seems to hinder NO formation.

Mayrhuber et al.[56] compared a rock ilmenite and a sand ilmenite, using both NH_3 and NO with syngas as fuel. NO formation was found to decrease with an increased temperature, and the mass-based conversion of the oxygen carrier needs to be above 0.99 to achieve NO formation. Further, the outgoing concentration of NO was approximately the same when adding NO and NH_3. The NO formation was investigated using two different approaches: one with alternating pulses of syngas and NO/NH_3, similar to Normann et al.,[54] and in the other, pulses of syngas together with NO/NH_3 were used. With this approach, it was possible to conclude that more NO was found in the presence of syngas, for the same degree of oxygen carrier conversion. This was clearly demonstrated for the addition of both NO and NH_3. This indicates that the syngas or H_2O and CO_2 formed by the syngas oxidation hinder the reduction of NO.

4.2. Nitrogen Compounds in Continuous CLC Operation. Song et al.[57] studied the conversion of fuel nitrogen in a 1 kW CLC unit using two coals and a Ni-based oxygen carrier. In the fuel reactor, all fuel nitrogen is converted to N_2 for both fuels. This agrees well with the lab reactor results of Normann et al.[54] above. However, NO was found in the air reactor as a result of the carryover of char. Song et al.[58]

also operated the 1 kW CLC unit with an iron ore, using bituminous coal and anthracite. Again, no NO was produced in the fuel reactor, while some NO is formed in the air reactor.

Markström et al.[59] conducted solid fuel operation with a 100 kW CLC unit using bituminous coal and ilmenite as the oxygen carrier. They found that typically 10−20% of fuel nitrogen is converted to NO. Also, NO increased when the oxygen demand decreased, e.g., at increased solids circulation. Further, increased addition of the steam fluidizing the fuel reactor led to a rise in NO formation.

Linderholm et al.[60] investigated NO formation in a 100 kW CLC unit with low-volatile solid fuels and ilmenite. With petcoke, they found that 3−8% of fuel nitrogen was converted to NO at 148 kW, while a 20% NO conversion was obtained at 72 kW. With wood char, fuel N conversion to NO was 7−32%. For both fuels, NO increased with solids circulation.

Linderholm et al.[61] made nitrogen balances for CLC operation in a 100 kW unit with a Columbian bituminous coal and ilmenite as the oxygen carrier and were able to account for 62% of incoming fuel nitrogen. Nitrogen converted into gaseous compounds had the distribution of 1% HCN, 11% NO, and 26% NH_3, with the remainder assumed to be N_2. In a later operation with a Polish coal[62] but with a mixture of ilmenite and manganese ore, the distribution was 0% HCN, 29% NO, and 11% NH_3. Higher NO is expected, because the oxygen demand was significantly lowered in the presence of manganese ore. Further, operation with Columbian coal and an iron ore in this unit found 10% NO and 37% NH_3.[63] Operation with Columbian coal and sintered manganese ore found 4−11% NO and 15−29% NH_3.[64] NH_3 fell and NO rose with rising circulation. Interestingly, NO was lower than in the previous cases, despite the fact that the oxygen demand was at a similarly low level as for ilmenite and manganese ore.

Mendiara et al.[65] operated a 500 W CLC unit with lignite as fuel and ilmenite. No N_2O was found, with only traces of NO_2, NH_3, and HCN. The only nitrogen compound other than N_2 found of any significant magnitude is NO. However, 99% of fuel nitrogen was converted to N_2 in the fuel reactor. NO_x emissions were found from the air reactor, from combustion of the unconverted char. Mendiara et al.[66] also investigated combustion of three biogenic fuels in the 500 W CLC unit with iron ore. They found similar nitrogen conversion to NO, 4−14%, for the three fuels used: sawdust, olive stones, and almond shells. NO was reduced at an increased temperature.

Gu et al.[67] examined the NO formation in a continuous 1 kW CLC unit with bituminous coal and iron ore. Using H_2O for fluidization, they found 24−68 ppm of NO from the fuel reactor, the highest concentration at the highest temperature, 980°C. A total of 0.5−0.8% of fuel N was oxidized to NO. At lower temperatures, NO from the air reactor was higher because of increased char loss from the fuel reactor.

Bayham et al.[68] investigated the behavior of a 25 kW coal direct chemical looping (CDCL) unit with a Fe-based oxygen carrier. CDCL is a similar process to CLC, albeit using a moving bed fuel reactor. They found that 10−15% of fuel nitrogen was converted to NO_x.

Ohlemüller et al.[69] found no NO from the fuel reactor when operating coal with ilmenite in a 1 MW CLC plant. The same result was found for a blend of iron ore and ilmenite. With iron ore only, 20 ppm was measured. With iron ore and a blend of coal and biomass, 8 ppm was found.

An overview of the operation where nitrogen compounds have been reported is given in Table 2.

4.3. Summary.
The literature shows that oxygen carriers can oxidize NH_3 to NO and that there are large differences between different oxygen carriers. The ability to form NO is not necessarily linked to the ability to oxidize fuel gases; for instance, highly reactive nickel oxide did not give any NO. The laboratory tests also shows that oxygen carriers can reduce NO. The ability to oxidize NH_3 and reduce NO is strongly linked to the degree of conversion of the oxygen carrier. Furthermore, CLC pilot operation shows that high concentrations of NO can form in the fuel reactor, despite the fact that equilibrium concentrations are very low. In addition, char leakage to the air reactor may form NO in the air reactor.

The purpose of this work is to expand the understanding of the NO_x chemistry in CLC, by investigating the fate of NO and NH_3 in a 300 W CLC pilot operated with gaseous fuel. This is accomplished by adding NO/NH_3 to the gas stream entering the fuel reactor.

5. MATERIALS AND METHODS

5.1. Linz−Donawitz (LD) Slag.
LD slag is a ground steel converter slag from the Linz−Donawitz process. Millions of tons of

Table 3. Elemental Composition of Fresh Oxygen Carriers Excluding Oxygen (wt %)

	Ca	Fe	Mg	Si	Mn	V	Ti
LS slag	27.3	13.7	6.0	4.8	2.2	1.6	0.7
ilmenite	0.2	34.5	2.2	0.9	0.2		26.9

LD slag are produced yearly, of which a large amount is disregarded and landfilled as waste with no further use. The major components that appear in LD slag are oxides of Ca (30−60%), Fe (10−35%), and Si (8−20%), with some amounts of Mg, Mn, Al, V, and Ti, depending upon the origin of the iron ore.[70] The low price and presence of iron

of LD slag could make it relevant for use in CLC. Moldenhauer et al.[71] investigated LD slag in chemical looping with syngas, methane, and biomass fuel. Full conversion of syngas at 900°C and 60% methane conversion at 950°C were obtained. CO_2 yields of 75−82% were achieved when operating with biomass fuel. LD slag was also used as bed material in the 12 MW circulating fluidized bed (CFB) boiler at Chalmers University of Technology to investigate oxygen-carrier-aided combustion (OCAC) with biomass.[72]

The LD slag was delivered by SSAB Merox, Sweden. The elemental composition of LD slag and ilmenite is given in Table 3. The oxygen carriers were calcined in air at 950°C for 24 h to ensure full oxidation. The calcined particles were sieved to obtain around 500 g of particles smaller than 212 μm, for use in the 300 W reactor.

5.2. Ilmenite.
Ilmenite has been subject to investigations in many studies related to CLC using various types of fuel since 2008,[73] and more than 1500 h of CLC pilot operation with ilmenite has been reported.[1] Ilmenite readily oxidizes syngas, with higher conversion of H_2 than CO.[74] However, the conversion of CH_4 is moderate.[73] Ilmenite is a low-cost natural iron titanium ore, which, in its natural state, mainly consists of $FeTiO_3$. This is also the reduced state. In the air reactor, ilmenite can be oxidized to its full oxidation state, according to

$$2FeTiO_3 + 1/2O_2 \rightarrow Fe_2TiO_5 + TiO_2 \tag{10}$$
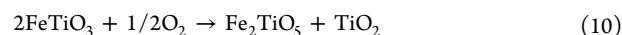
Just like LD slag, ilmenite has been used in OCAC, including 20 000 h of burning municipal solid waste in a 75 MW CFB boiler.[75−77]

5.3. Chemical Looping Fluidized Bed Reactor System at 300 W.
The experiments were performed in a dual fluidized bed 300 W CLC reactor system, with syngas fuel under continuous circulation of oxygen carrier particles. The schematic illustration of the 300 W chemical looping reactor used in this work is shown in Figure 6.

The reactor is 300 mm high, with a cross section of 25×25 mm for the fuel reactor (FR) and 25×42 mm for the air reactor (AR). The riser of the AR is 25×25 mm and is operated at a gas velocity sufficient to transport the particles upward, thus accomplishing the circulation of bed material. There is a gap between the two reactors to secure that no gas can leak between them. There are two wind boxes located in the bottom of each reactor to inject the gas via porous quartz plates, which act as gas distributors. There is a top part above both reactors, where the cross section of the gas path widens and gas velocity consequently decreases, allowing elutriated particles to fall back into the reactors. On the AR side, the section is designed to lead part of the particles into a loop seal that connects the AR to FR. On the FR side, particles drop directly back into the FR. From the bottom of the FR, particles pass through the lower loop seal and return to the AR, where the cycle starts over, completing the loop. The two loop seals are fluidized with inert gas, a total of 0.65 L_n/min of argon, when operating with fuel to ensure the fluidization and circulation of the particles. The exit pipe of the FR is connected to a water seal with a column height of less than 20 mm to maintain a slightly higher pressure, 0.1−0.2 kPa, in the FR compared to AR to minimize the risk of gas leakage from AR to FR. The bed temperatures of the AR and FR are measured by means of K-type thermocouples. The 300 W reactor is located inside an electrical furnace that controls the temperature. The fluidization and circulation of the particles are monitored via pressure difference measurement at different heights of the AR and FR.

5.4. NH_3 Measurements.
The setup was devised to make it possible to measure ammonia directly using Dräger tubes. To avoid the dissolution of ammonia in condensed water, the gas stream must be dried while still being above the point of condensation. Further, the drying of the gas must not remove any ammonia. Therefore, the moist hot gas stream was passed over a desiccant, i.e., sodium hydroxide (NaOH), which is a strong base at the same time, allowing water vapor to be absorbed, while ammonia leaves the drying unit unreacted. A stream of gas from the FR was led through the drying step. This stream was well-insulated and heated to stay above 100°C to avoid any water condensation. After drying, a Dräger tube is used to measure the concentration of ammonia in the dry gas stream. The
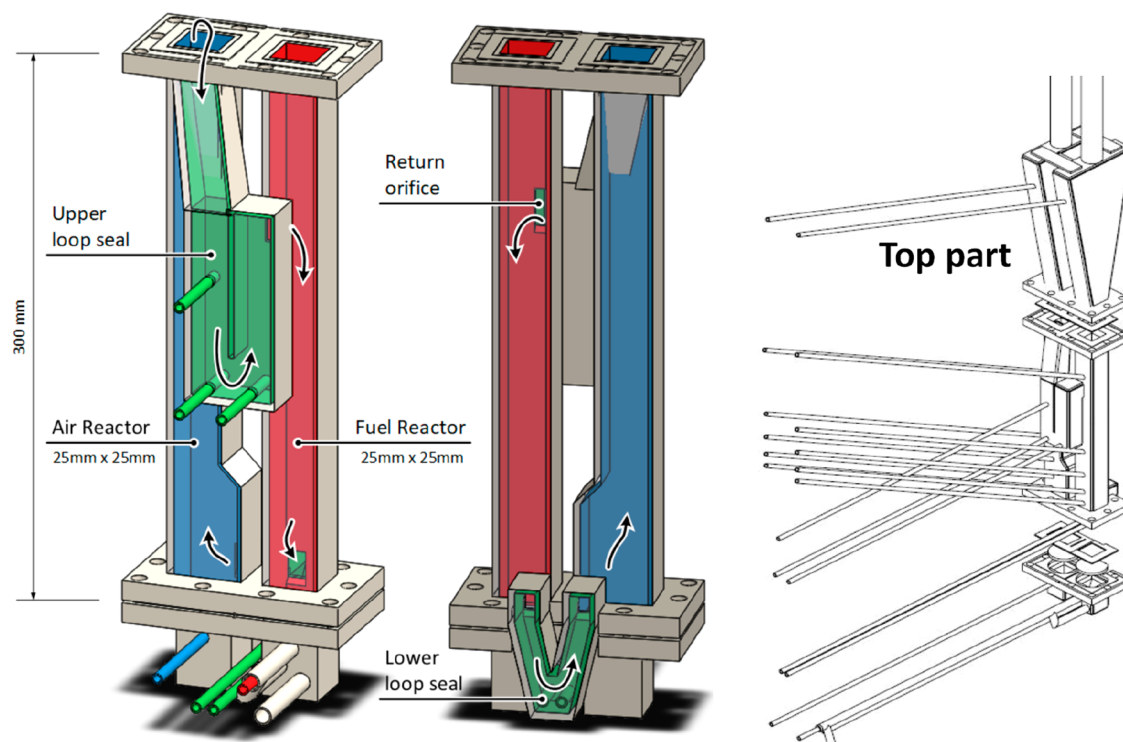
Figure 6. (Left) Back and front view of the 300 W reactor[78] and (right) system with the top part.[79] This figure was reproduced with permission from ref 80. Copyright 2022 Elsevier.
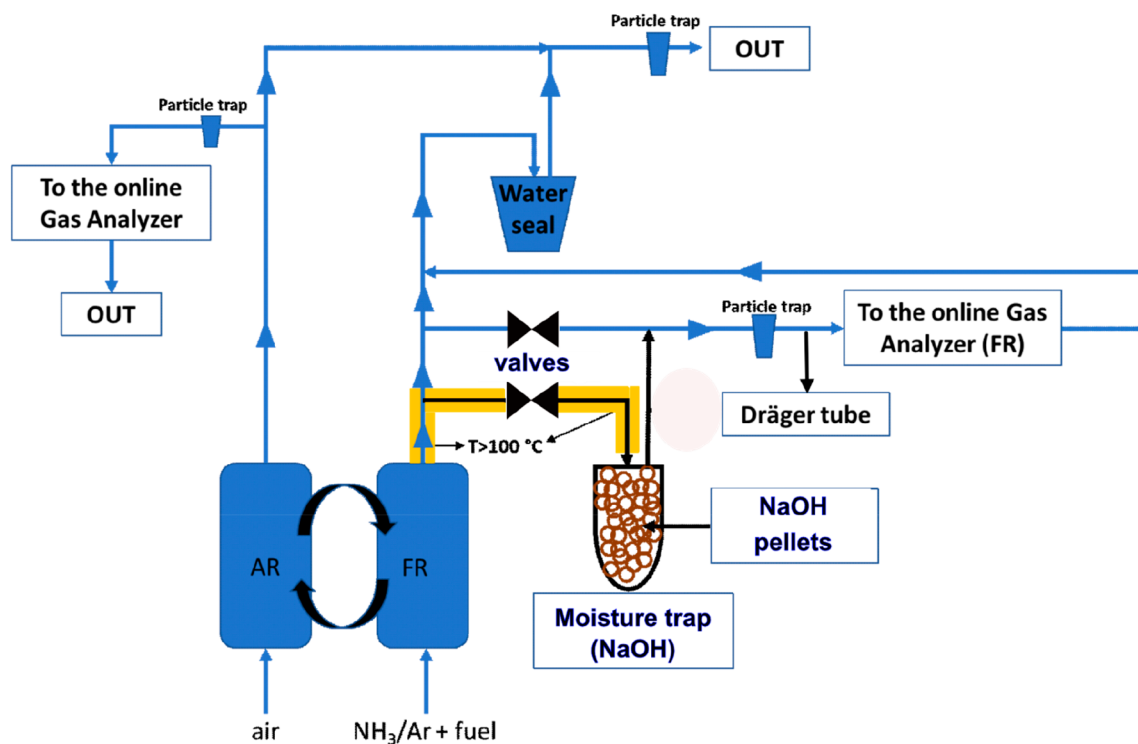

Figure 7. Setup for NH_3 measurements.

setup included a valve that was opened for 5 min for each measurement.

The reactor is run with syngas at a maximum flow of 1 L_n/min. Assuming that the syngas conversion to steam and CO_2 is 100% and that all of the flue gas is led through the drying unit for 5 min, 9 g of sodium hydroxide in total is needed for the reaction with CO_2 and

absorbing water. On the basis of this, adequate amounts of drying agent were added to the moisture trap and exchanged regularly. Although CO_2 reacts with hydroxide, it does not interfere with the procedure because there will be enough hydroxide in the drying unit to keep the pH very low and, thus, prevent reaction with ammonia. Figure 7 shows a schematic plan of the setup. The online gas analyzer
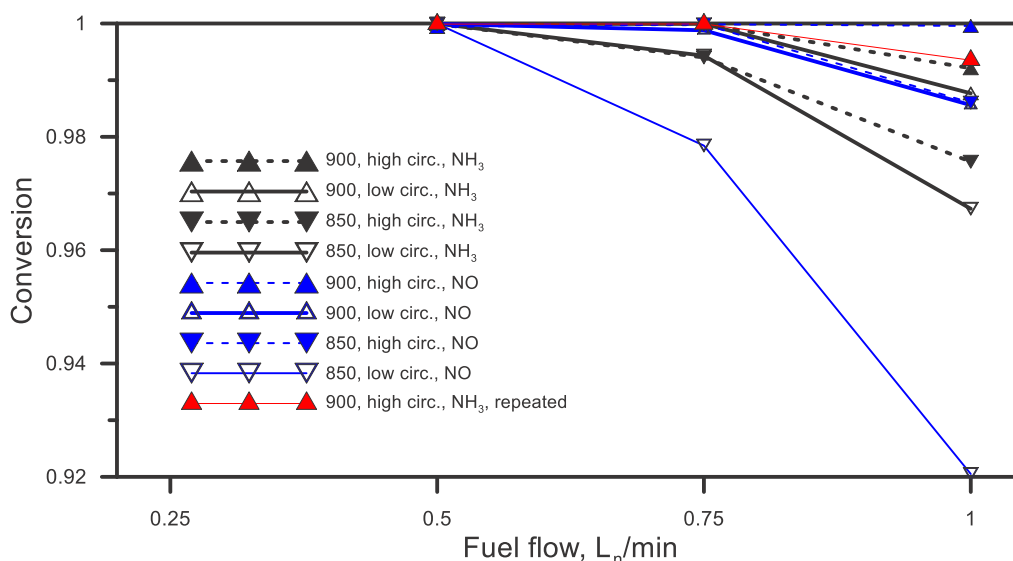
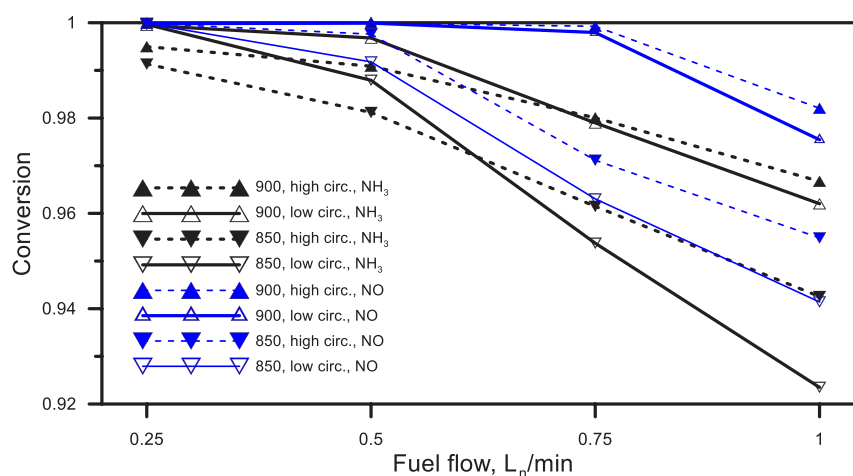**Figure 8.** Conversion versus fuel flow for LD slag.

Figure 9. Conversion versus fuel flow for ilmenite.

is equipped with a pump that sucks 1 L_n/min. With the opening of the valve leading to the moisture trap and closing of the other valve leading to the gas analysers, the gas is forced through the moisture trap and can be sampled by Dräger tubes.

5.5. Circulation. The solids circulation was estimated using the char injection method,[81] whereby 0.5 g of char was added to the fuel reactor and the circulation is derived from the response in the CO_2 concentration from the air reactor. For each oxygen carrier, two air flows were used in the air reactor, 8 and 9 L_n/min, giving two different circulations below called high and low. For LD slag, the low and high circulations were 120 and 144 g/min, and for ilmenite, they were 75 and 84 g/min.

The solids inventory of the fuel reactor was estimated to 100 g for LD slag and 95 g for ilmenite, corresponding to a residence time in the fuel reactor of somewhat below 1 min for LD slag and a little more than 1 min for ilmenite.

5.6. Experimental Procedure. Prior to the experiments, oxygen carriers were activated with syngas, 50% hydrogen in CO, at 900°C for 2−3 h. Oxygen carriers were circulating during the activation, and the air flow rate to the AR was 8 L_n/min. Reaching a stable concentration of CO_2 from the FR was used to confirm the activation.

The study involved the addition of a stream of NO or NH_3, diluted in argon, to the fuel reactor, normally at a concentration of 1% but in a few cases at 0.2%. The tests involved the addition of these flows to the fuel reactor during chemical looping operation of the 300 W

reactor system, normally together with fuel and in some cases also an additional inert flow. Further, a part of the inert gas from the fluidization of the loop seals also mixes into the gas stream in the fuel reactor. Normally, the air reactor was fluidized with air that was diluted with gas from the loop seals. The test matrix involved two oxygen carriers, two temperatures, two circulation flows, and three or four fuel flows.

Furthermore, experiments were made without fuel addition as well as with an empty reactor system.

5.7. Data Evaluation. Gas conversion of the syngas was based on the CO conversion to CO_2, because H_2 was assumed to be essentially complete for these tests. Thus, gas conversion was attained as

$$\eta_{gas} = 1 - \frac{x_{CO}}{x_{CO_2}}$$

(11)

where x_i is the volumetric concentration of species i.

6. GAS CONVERSION IN CHEMICAL LOOPING OPERATION

The work involved almost 20 h of fueled operation with LD slag as well as almost 20 h with ilmenite. Figure 8 shows the gas conversion in operation with LD slag with either NH_3 or NO addition. Conversion was complete for the lowest fuel flow. As expected, it was higher for a high temperature and

high circulation. The trends are similar for the tests with NH_3 and NO. Given the small amount of NO or NH_3 added, similar results would be expected for both cases. There is no consistent difference: in two cases, the tests with NO show higher conversion, and in the other two cases, they show lower or slightly lower conversion.

Similarly, the gas conversion for ilmenite is shown in Figure 9. It is clear that the conversion is somewhat lower than for LD slag, but in all cases, the gas conversion is above 92%. The difference is more pronounced at lower fuel flows, e.g., 0.5 L_n/min, where LD slag has full conversion in all cases, whereas ilmenite only shows full conversion in one case. A possible explanation could be that LD slag has higher reactivity but lower oxygen transfer capacity. It is also evident that the temperature has a larger impact on conversion for ilmenite. Similar to LD slag, higher circulation is consistently giving higher conversion.

7. NH$_3$ TESTS WITH AN EMPTY REACTOR

To validate the measurement procedure, measurements were made with an empty reactor, i.e., in the absence of an oxygen

Table 4. Gas Concentrations Measured

sample	T (°C)	NH_3 (ppm)	H_2 (%)	NO (ppm)
1	900	15	0.1	0
2	900	15	0.12	0
3	900	50	0.13	0
4	900	70	0.19	0

carrier. The investigation involved the addition of NH_3 in argon, at both varying the temperature and constant temperatures of 850 and 900°C

7.1. Empty Reactor with NH$_3$: Temperature Ramping. The reactor temperature was increased gradually while 1.5 L_n/min of 1% NH_3 in argon was added to the fuel reactor. The aim was to observe when ammonia starts to decompose in the fuel reactor. Below 625°C, the measured level of NH_3 was 1%, i.e., 10 000 ppm, and hydrogen was 0%. However, at 625°C, NH_3 decreased to 9500 ppm and 0.1% hydrogen appeared. At 700°C, NH_3 dropped to 15 ppm and the gas chromatograph

(GC) showed 0.3% nitrogen, indicating the breakdown of NH_3 to N_2 and H_2. When the temperature reached 850°C, hydrogen was 0.31% and NH_3 was still 15 ppm.

7.2. Empty Reactor with NH$_3$: Stable Temperature of 900 and 850°C. NH_3 was added while the empty reactor was stable at 900°C to observe the decomposition of ammonia. The added flow was higher than in the temperature ramping, 1.5 L_n/min of 1% NH_3 plus 1 L_n/min of pure argon, thus giving 6000 ppm. Concentrations were measured every 5 min, and the results are shown in Table 4.

The temperature was then lowered to 850°C, and a stable concentration of 55 ppm was seen, while the GC found 0.36% hydrogen.

Thus, around 99% of ammonia breaks down at both 850 and 900°C. This is consistent with thermodynamic equilibria, showing that both NO and NH_3 have negligible concentrations in the absence of oxygen (see Figure 5). However, the expected concentration of H_2 for breakdown to N_2 and H_2 would be 0.9%, but measured values are 10−20% of that. A possibility could be that H_2 reacts with the reactor walls.

The residence time of the gas in the wind box and the pipe leading to the windbox is small compared to the residence time in the reactor and the top part above the reactor. In addition, the incoming gas is cold, and the wind box is cooled; therefore, it is likely that the major breakdown of ammonia takes place after entering the fuel reactor. Consequently, it is assumed that all or a major part of ammonia reaches the bed of the oxygen carrier in the tests below.

8. EXPERIMENTS WITH LD SLAG

8.1. Tests with NO or NH$_3$ without Fuel. A total of 1% of NH_3 in argon was added to the fuel reactor, while the oxygen carrier was circulated between the air and fuel reactors at two different temperatures, 850 and 900°C. It was found that 6−10% of NH_3 was oxidized to NO. A high circulation and high temperature gave higher conversion to NO. There was no NH_3 in the gas sampled.

Similarly, 0.2% of NO was added to the fuel reactor. The NO concentration measured corresponded to 87−93% of incoming NO. The numbers were lower for 900°C and also lower for high circulation. It can be concluded that a majority
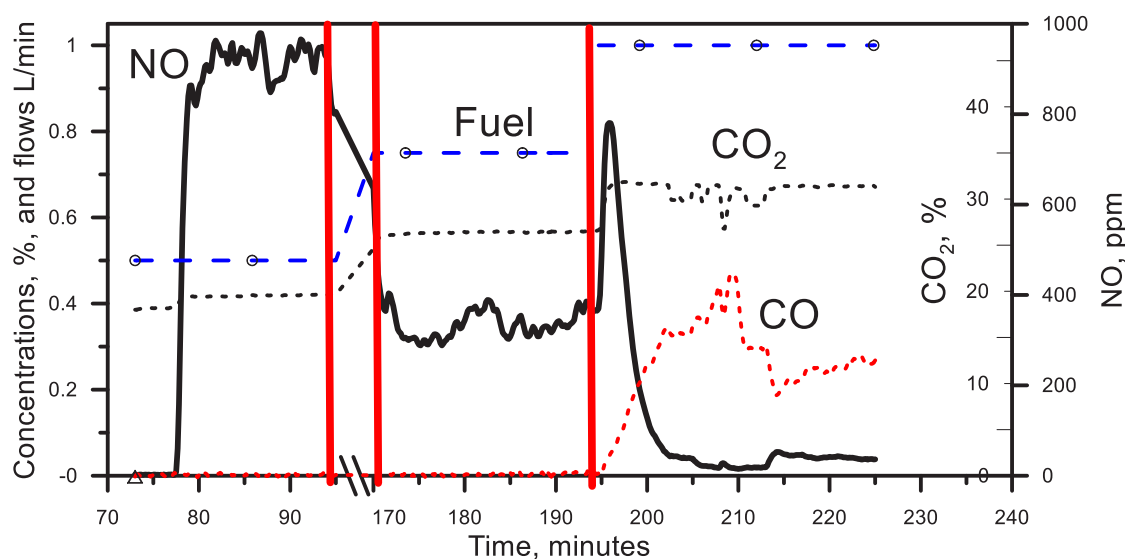

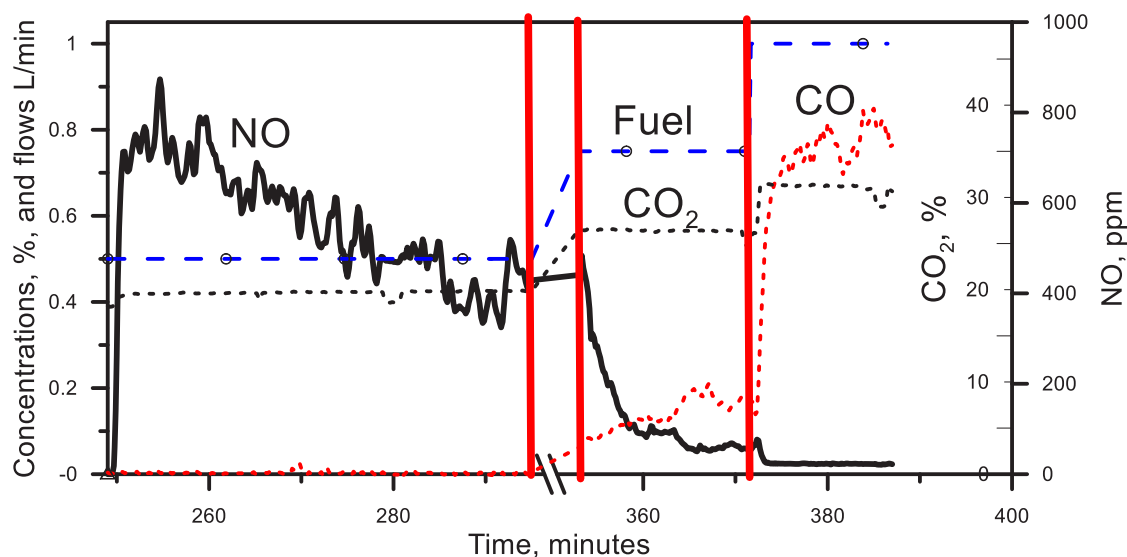**Figure 10.** NH$_3$ addition at 900°C and high circulation.

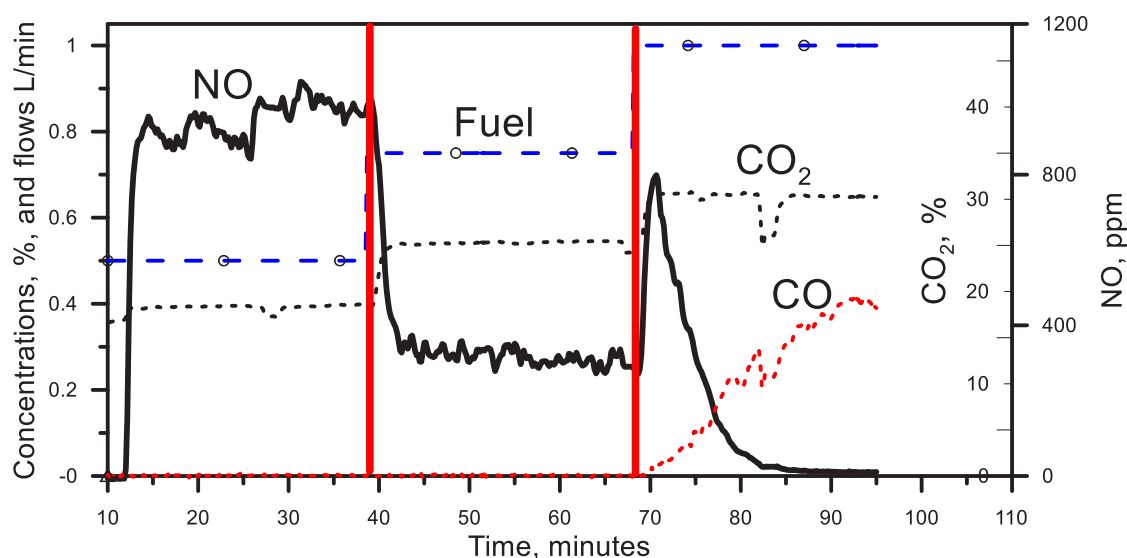**Figure 11.** NH_3 addition at 850°C and high circulation.

Figure 12. NH_3 addition at 900°C and low circulation.

of NO passes through the fuel reactor when the oxygen carrier is fully oxidized. NO is not expected to be reduced by the fully oxidized oxygen carrier. The deviation from 100% could be a result of error in the mass balance. When bed material is circulated, inert gas is added to upper and lower loop seals and a part of the gas goes to the air reactor, while the rest of the gas goes to the fuel reactor. Thus, the gas to the fuel reactor is diluted with this flow, and the mass balance will be dependent upon the assumption of the gas fraction going to the fuel reactor. This fraction may also be affected by the temperature, solids circulation, and pressure difference.

8.2. Tests with LD Slag, Fuel, and NH_3. Figures 10−13 show the effect of the temperature, fuel flow rate, and circulation rate on the NO emissions with the addition of 10 000 ppm of NH_3 in argon. The argon/NH_3 flow was 1 L_n/min, and the syngas flow is shown in the diagrams. Further, the inert gas added to the loop seals is assumed to give an additional 0.42 L_n/min. Three syngas flows were used, 0.5, 0.75, and 1 L_n/min, which means that NH_3 was diluted by a factor of 1.9−2.4 depending upon syngas flow. Figures 10 and

11 show the results for the higher solids circulation. The highest conversion of NH_3 to NO was obtained for the lowest fuel flow, where around 17% is converted to NO at the higher temperature and 8% is converted to NO at the lower temperature. On the other hand, there was little NO at the highest fuel flow. This is also expected because higher fuel flows mean a more reduced oxygen carrier with reduced ability to oxidize NH_3 to NO. The results for the lower circulation (Figures 12 and 13) are fairly similar to the higher flow. Several of the shifts to higher fuel flow are accompanied by a peak in NO. The cause for this peak is not clear, but the peak subsides as CO gradually increases after the shift. The increase in NO when CO again decreases at 215 min should also be noted (Figure 10). Also, Figures 11−13 show how decreases in NO are associated with increases in CO. For CO concentrations above 0.2−0.3, the NO concentrations are very low.

The results are summarized in Figure 14, including data for no fuel addition. The data for fuel addition were each collected in sequence on the same day, whereas the data for zero fuel flow were collected at a later date. The lower oxidation for NO
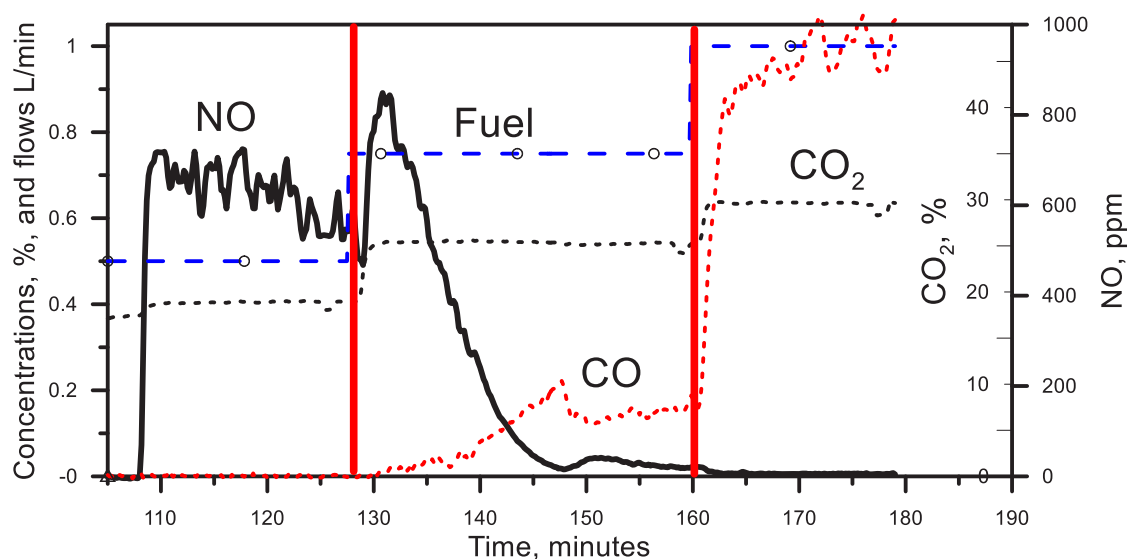
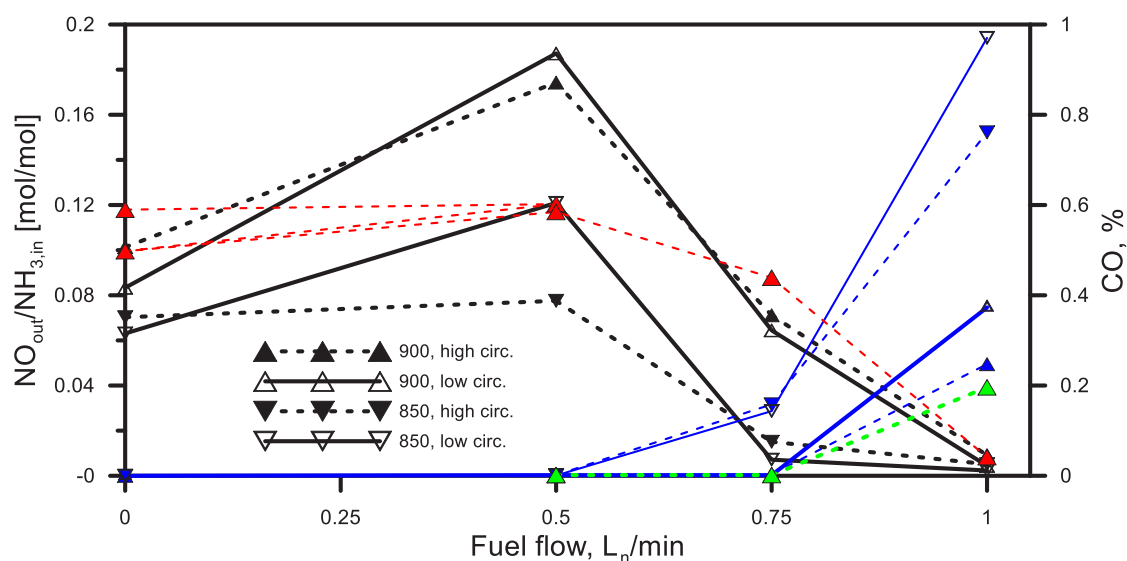**Figure 13.** NH_3 addition at 850°C and low circulation.

Figure 14. NO and CO versus fuel flow for the addition of 1 L_n/min of 1% NH_3 in argon, with NO in black and CO in blue, and an additional test at 900°C with high circulation in red (NO) and green (CO).

in the absence of fuel is somewhat unexpected and may possibly be an artifact explained by some difference in the experimental conditions, e.g., lower bed content because of the loss of particles or loss in reactivity. However, an additional test series was made at 900°C with high circulation, where the fuel flow was varied from zero the same day, with the following sequence of fuel flow: 0, 0.5, 0.75, 1, 0, 0.5, 1, and 0. The sequence is shown in red in Figure 14, and there is no significant difference between no fuel and 0.5 L_n/min, which should be noted. In contrast to the test in Figure 10, this sequence was operated with a constant gas flow of 2 L_n/min to the fuel reactor. While the flow with NH_3 was constant at 1 L_n/min, lower fuel flows were compensated by the addition of argon. Thus, for flows other than 1 L_n/min, both fuel and NH_3 are more diluted in comparison to the other tests. The general expectation of course is that a higher state of oxidation would promote the oxidation of NH_3 to NO. However, the detailed reaction paths are not known, and the presence of fuel also involves the presence of high concentrations of steam and

CO_2, which could potentially promote NO formation or hinder reduction of NO. As previously noted, Mayrhuber et al. found increased conversion of NH_3 to NO in the presence of syngas, for a similar degree of oxidation of the oxygen carrier ilmenite.[56]

However, with the spread in the data, no safe conclusion can be made whether the formation of NO really increases when going from no fuel flow to low fuel flow, i.e., 0.5 L_n/min.

There is a clear decrease in oxidation to NO as more fuel is added. Conversion to NO is consistently higher at a higher temperature, whereas the effect of circulation is small.

The oxidation to NO is strongly correlated to the CO concentration, as shown in Figure 15. In the presence of CO, there is essentially no formation of NO, whereas in the absence of CO, the formation of NO is significant in all cases.

8.3. Tests with LD Slag, Fuel, and NO. Figures 16 and 17 show the effect of the fuel flow rate and circulation rate on the NO emissions with the addition of 10 000 ppm of NO in argon at 900°C. The argon/NO flow was 1 L_n/min, and the syngas
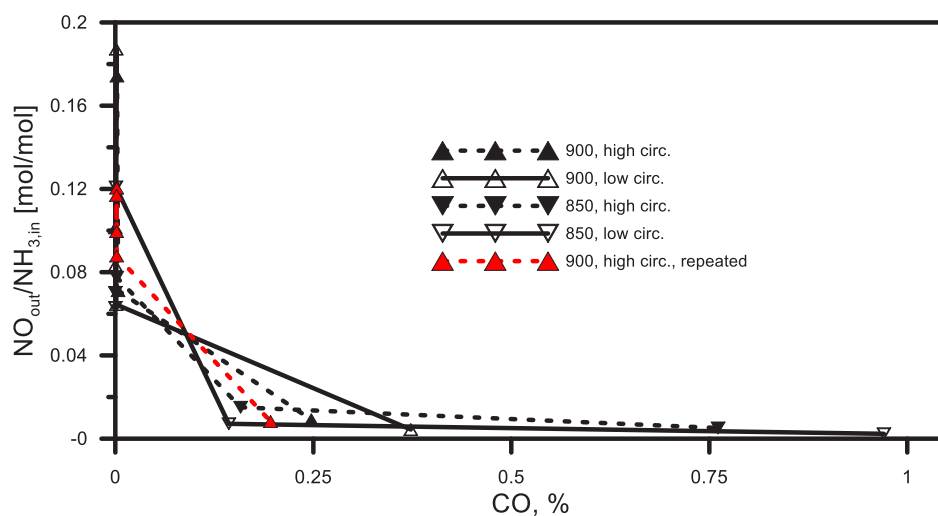
Figure 15. NO and versus CO for the addition of 1 L_n/min of 1% NH_3 in argon.
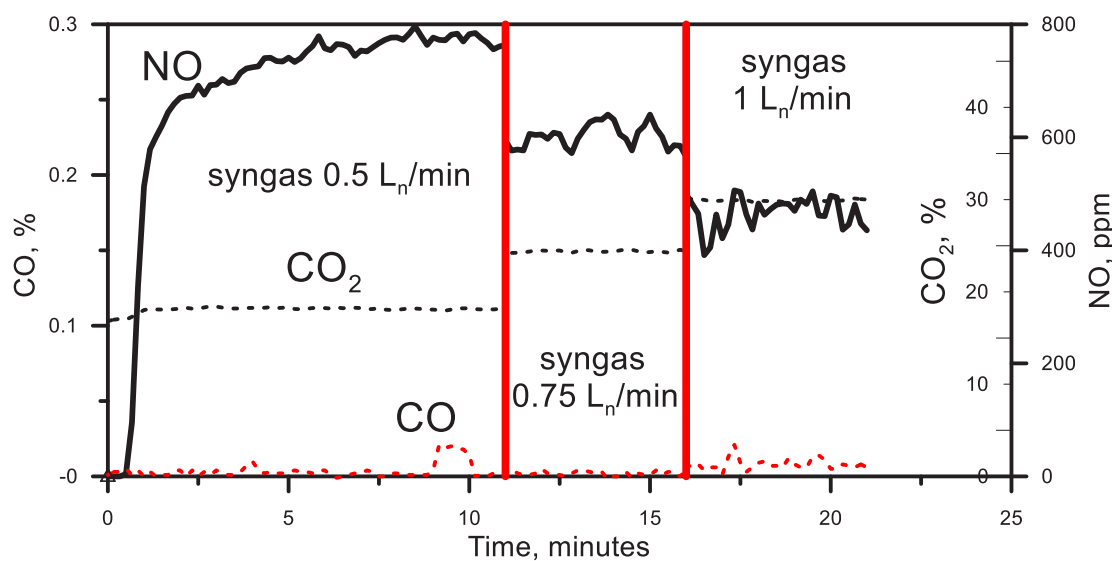

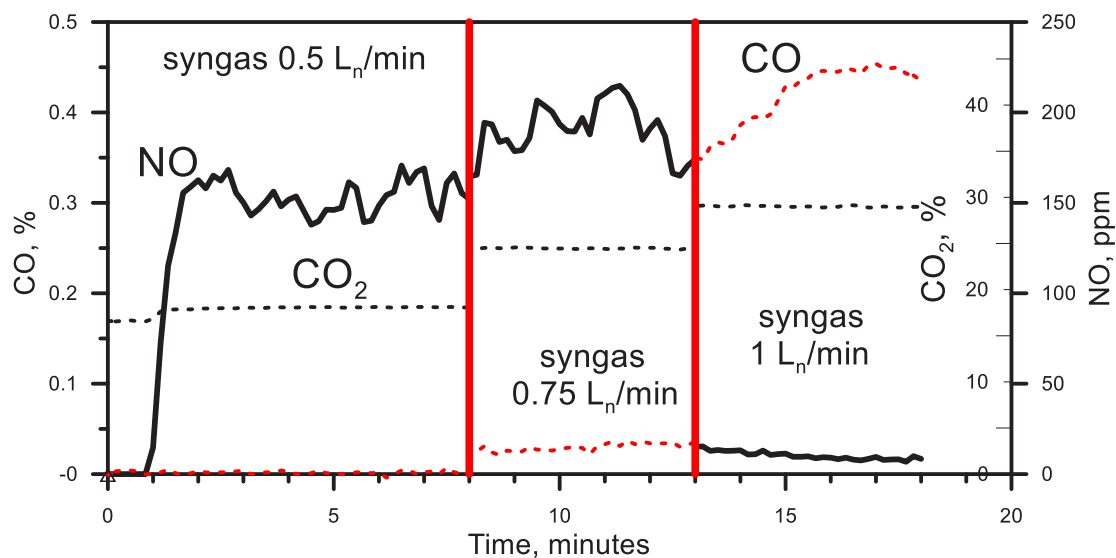**Figure 16.** NO addition at 900°C and high circulation.

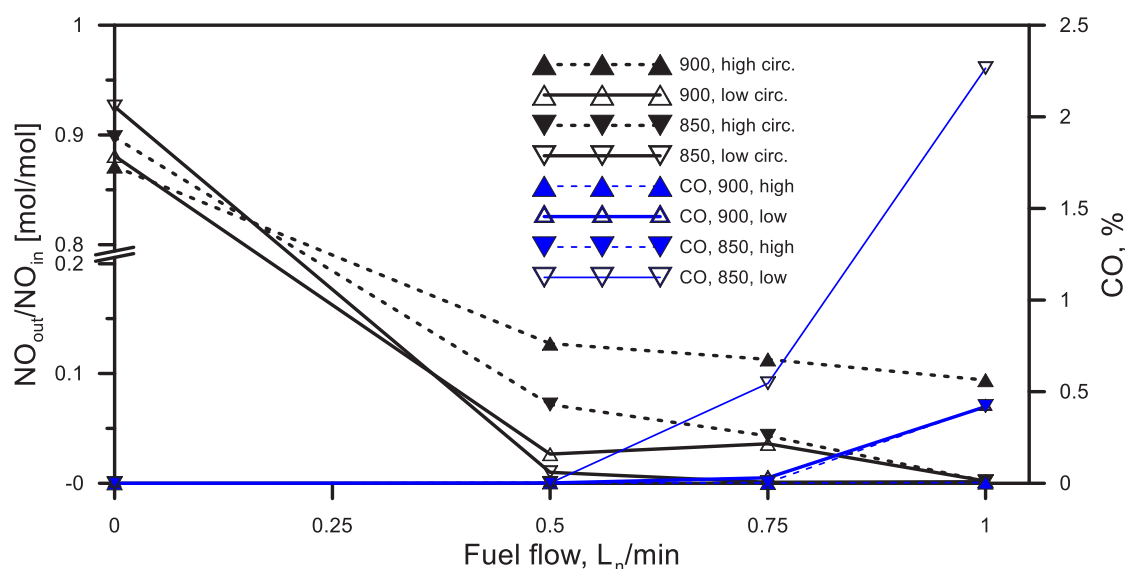**Figure 17.** NO addition at 900°C and low circulation.

Figure 18. NO and CO versus fuel flow for the addition of 1 L_n/min of 1% NO in argon together with various fuel flows.
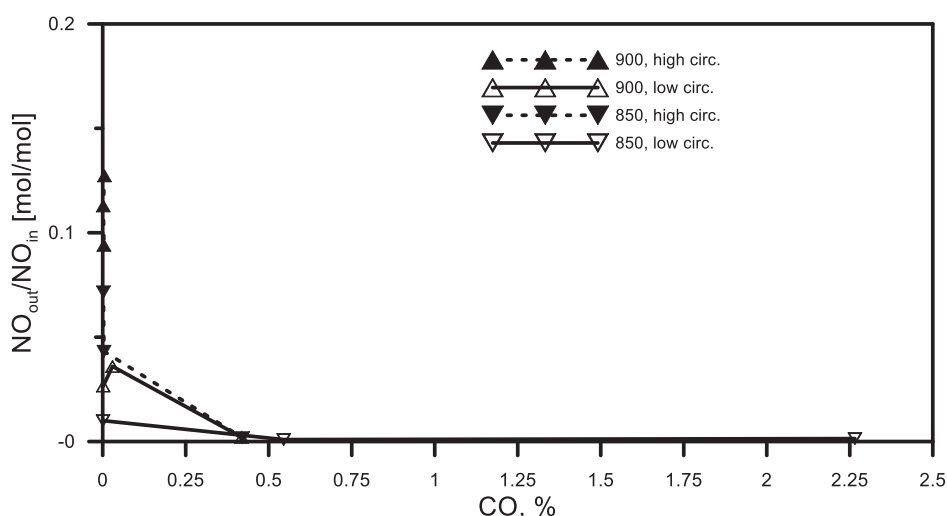

Figure 19. NO and versus CO for the addition of 1 L_n/min of 1% NO in argon.

flow is shown in the diagrams. Further, the inert gas added to the loop seals is assumed to give an additional 0.42 L_n/min. Three syngas flows were used, 0.5, 0.75, and 1 L_n/min, which means that NO was diluted by a factor of 1.9−2.4 depending upon syngas flow. It is clear that the reduction of NO increases when more syngas is added.

Similar results are found at 850°C, although the breakdown of NO is higher at lower temperatures.

The results are compared in Figure 18. It is clear that lower circulation and higher fuel flow give increased reduction of NO. This is expected; more syngas and lower circulation should both contribute to give a more reduced oxygen carrier as well as higher concentration of reduced gaseous species. It is also clear from the figure that a lower temperature is associated with a higher breakdown of NO. At a lower temperature, the CO concentration is also higher.

Normally, a lower temperature is associated with slower reactions, but there are two possible explanations for this. Either the presence of CO enhances the breakdown, or the surface of the oxygen carrier is more reduced, e.g., as a

consequence of less rapid transfer of oxygen inside the oxygen carrier. The latter then also explains higher CO.

Figure 19 shows the correlation between NO and CO for the tests shown in Figure 18. It is clear that, in the presence of CO, the breakdown of NO is complete, whereas in the absence of CO, at least some NO escapes through the bed.

8.4. Addition of NO and NH_3 in the Absence of Fuel but with Reduced Oxygen Carrier Particles. From the studies with the addition of fuel, it is clear that oxidation of NH_3 to NO is lower in the presence of fuel. The experiment shown in Figure 20 was performed to see whether the reduced oxygen carrier is able to oxidize NH_3 to NO also in the absence of fuel. The temperature was 900°C, and the gas flow to the air reactor was set to give high circulation. Initially, the 300 W CLC unit was operated with syngas. Then, the air flow to the air reactor is changed to argon, thus ending the regeneration of the oxygen carrier coming from the fuel reactor. For 2 min, the system is run with continued syngas flow and no air flow, thus reducing the oxygen carrier. After 2 min, the syngas flow is stopped, and with only inert gases added, the reduced state of the oxygen carrier is preserved. A few minutes later, NH_3
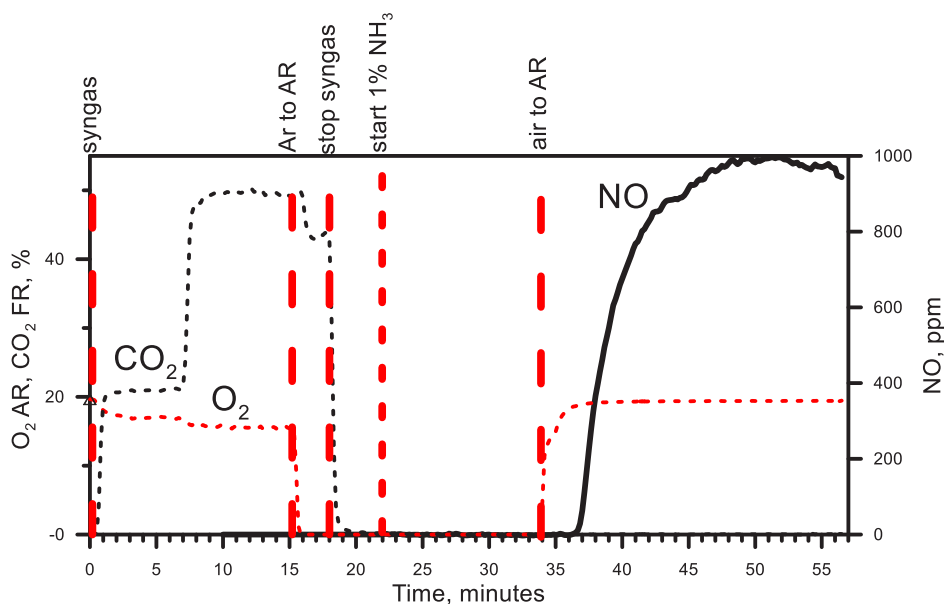
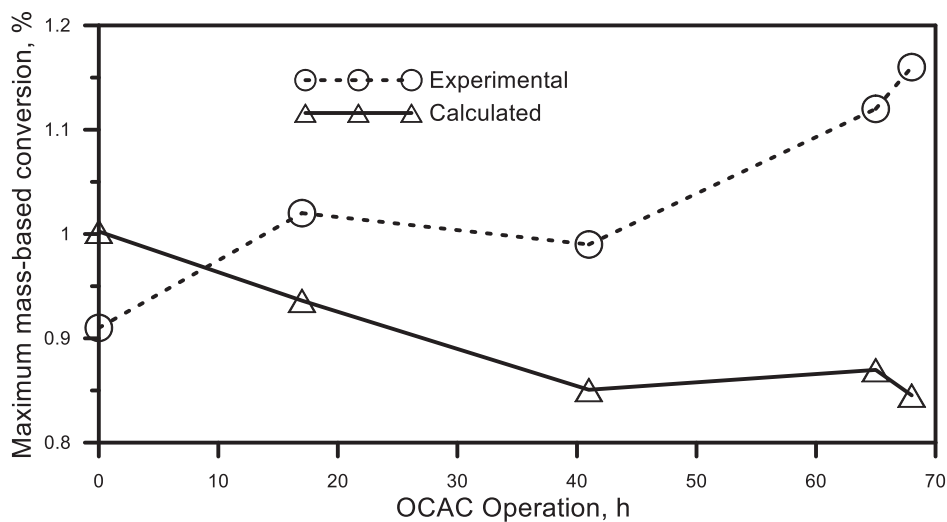**Figure 20.** Adding NH_3 without fuel but after reducing the LD slag.

Figure 21. Maximum mass-based conversion of LD slag. Data were from ref 70. The first sample at 0 h was oxidized for 24 h before investigation.

addition is started, and it is clear that there is no oxidation of NH_3 to NO. After 12 min, feeding of air to the air reactor commenced, and 3 min later, NO starts to rise and stabilize at around 1000 ppm of NO, which corresponds to a conversion of NH_3 to NO of 15%.

The 2 min without regeneration only gives a partial reduction of the oxygen carrier, which should be noted. Thus, the gas conversion is essentially complete during the 2 min, and only at the end of the 2 min, a minor peak of 0.1% CO_2 was seen. This is not shown in the figure. A syngas flow of 1 L_n/min during 2 min will remove 1.4 g of oxygen from the oxygen carrier. Assuming approximately 500 g of oxygen carrier, this means a reduction in mass-based conversion of approximately 0.3%. However, the oxygen carrier is not fully oxidized when the 2 min period starts, which means that the mass-based reduction is higher than 0.3%. This can be compared to the theoretical maximum mass-based conversion of LD slag of around 1%[70] (see Figure 21). The theoretical maximum seems to be below that determined from experiments. It is not clear why, but it may possibly be associated

with the formation of various mixed oxide phases involving Fe, Ca, Si, Mn, and Al.

Similar to the test above, where it was examined whether the partly reduced oxygen carrier could oxidize NH_3, it was examined whether the partly reduced oxygen carrier could reduce NO. The test is shown in Figure 22, and again, a period of 2 min of reduction of the oxygen carrier is made. A few minutes after this, the addition of gas containing NO is started. It is evident that all NO is converted. Several minutes later, air addition to the air reactor is started, and after some delay, the reduction of incoming NO stops and the NO concentration quickly exceeds the maximum concentration range of the NO analyzer, explaining the plateau at 2400 ppm. At this point, the concentration of NO in the inlet gas is lowered to 0.2%, i.e., 2000 ppm. Bearing in mind that the gas is diluted with gas coming from the loop seals, the NO concentration then stabilizes at a level that is reasonably close to that expected with no reduction.
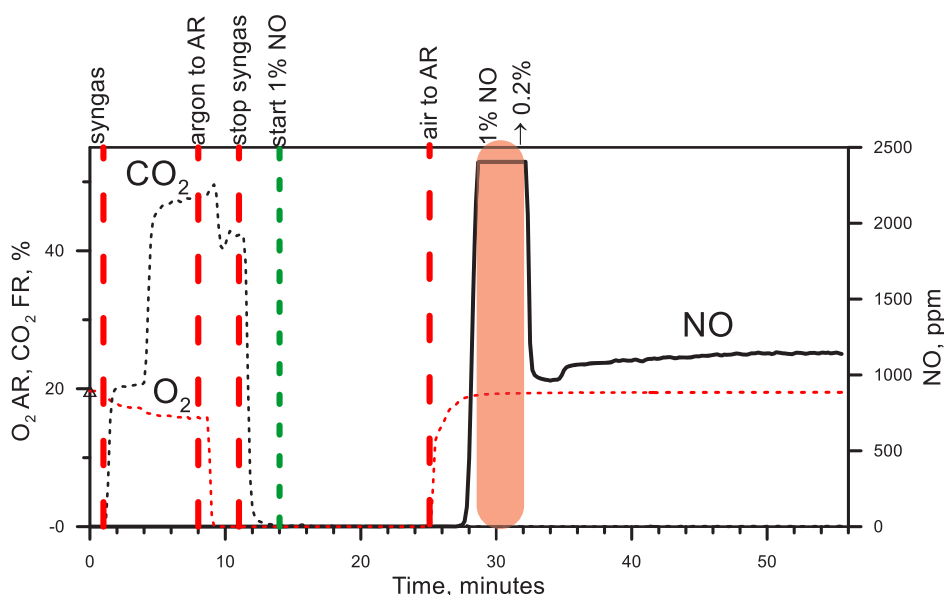
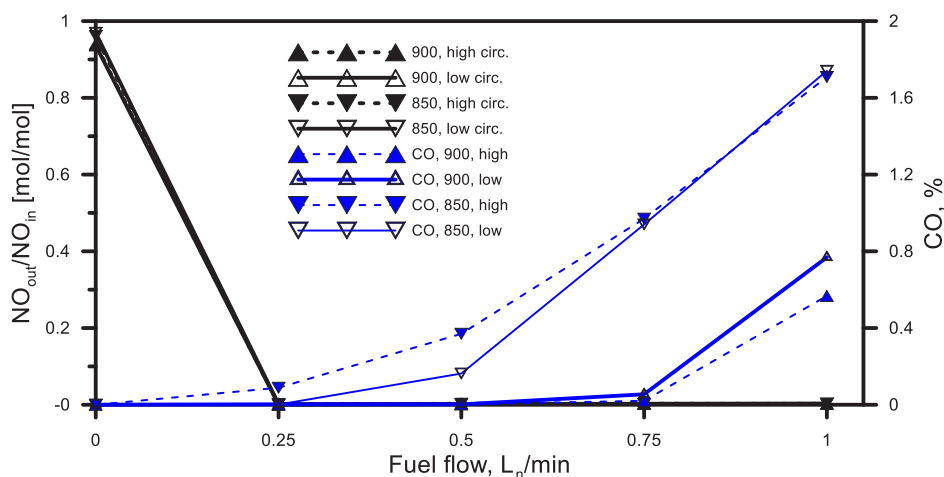**Figure 22.** Ability of reduced LD slag to reduce NO in the absence of fuel.

Figure 23. NO and CO versus fuel flow in operation with ilmenite with the addition of 1 L_n/min of 1% NH_3 in argon.

9. EXPERIMENTS WITH ILMENITE

9.1. Tests with Ilmenite and NH_3, with and without Fuel. Similar to the experiments with LD slag, the effect of fuel flow on the oxidation of NH_3 was investigated for ilmenite. The test matrix was expanded with an additional low flow, 0.25 L_n/min, which is half of the lowest flow used for LD slag. In contrast to the LD slag results, no significant conversion of NH_3 to NO was found for any of the fuel flows. The results are summarized in Figure 23. The levels of NO in the presence of fuel are all below 0.4% of added NH_3, which is also below 1% of the measurement range of the analyzer. The very low levels measured are believed to be an artifact caused by cross sensitivity with CO, which could also explains the consistent increase in NO with fuel flow. It can be concluded that NO levels during all cases of fuel addition are very low and below the detection limit.

9.2. Tests with NH_3 and Ilmenite with No Fuel but with a Reduced Oxygen Carrier. To examine whether the oxygen carrier in its partly reduced form but in the absence of fuel is able to oxidize NH_3 to NO, the oxygen carrier was reduced before introducing NH_3. The procedure is similar to

the test LD slag previously shown in Figure 20 and is shown in Figure 24. First, syngas is added to the fuel reactor, and then air addition to the air reactor is stopped, while fuel addition is allowed to proceed for another 2 min to reduce the oxygen carrier. The CO concentration during fuel addition, not shown, was 0.5−0.6% both before and after turning off the air. After the stop of fuel addition, the reduced state is conserved because only inert gas is added to the air and fuel reactors. After a few minutes, the addition of NH_3 to the fuel reactor is started. The figure clearly indicates that the reduced oxygen carrier cannot oxidize any NH_3 to NO. After 3 min of NH_3 addition, fluidization of the air reactor is shifted from argon to air. Oxidation of NH_3 only starts after several minutes of air addition to the air reactor and then slowly increases. Thus, the figure indicates that oxidation to NO only happens when ilmenite is highly oxidized.

In comparison to the results shown with LD slag (Figure 20), it is clear that the return of the ability to oxidize NH_3 is much slower for ilmenite. An important difference between ilmenite and LD slag is that the maximum mass-based conversion of ilmenite is significantly higher, 5% for pure
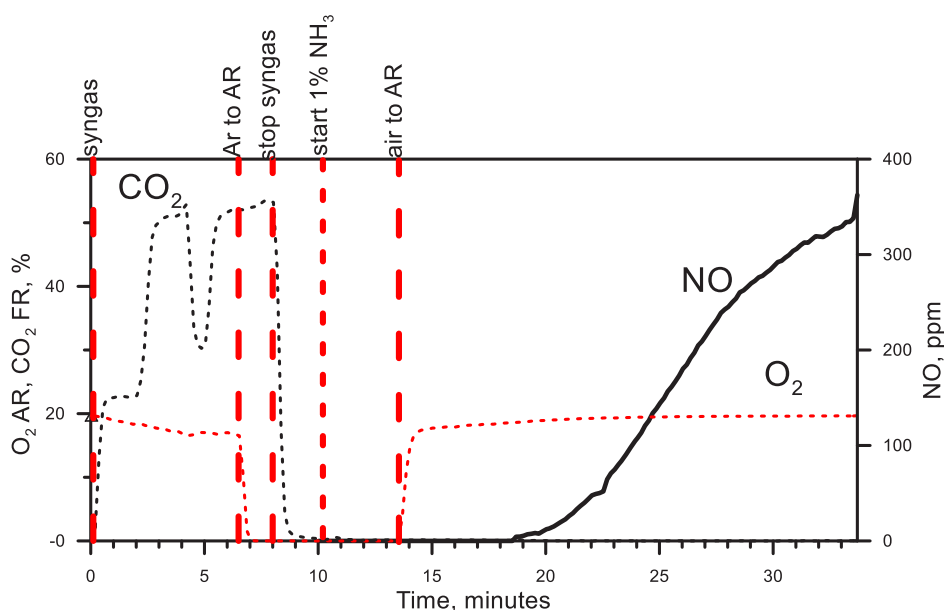
Figure 24. NH$_3$ addition to a bed of reduced ilmenite in the absence of fuel.
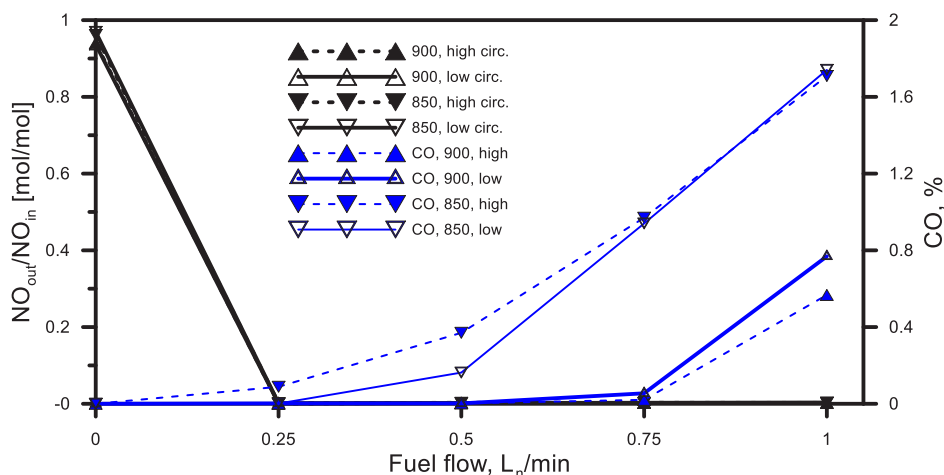

Figure 25. NO and CO versus fuel flow for the addition of 1 L$_n$/min of 1% NO in argon together with various fuel flows.

ilmenite and 1.7% for fully phase-separated iron and titania oxides.[82] The maximum mass-based conversion of ilmenite in actual operation is likely in the range of 3−4%. However, in both cases, the oxygen carrier was reduced for 2 min, which should give a similar change in mass-based conversion. However, the mass-based conversion at the starting point of the reduction is not necessarily the same.

9.3. Tests with Ilmenite and NO, with and without Fuel. Similar tests with and without fuel flow and a flow of 1 L$_n$/min with 1% NO were made. Figure 25 shows the ratio of NO$_{out}$/NO$_{in}$ versus fuel addition. Within the uncertainty of the mass balance, it can be said that, in the absence of fuel, all NO seems to pass through the bed, but in the presence of fuel, all NO is reduced independent of the fuel flow, temperature, or circulation. In all cases, measured NO$_{out}$/NO$_{in}$ is 0.003 or lower. Just as with NH$_3$ addition previously shown in Figure 23, there is a slight increase with fuel flow, which is believed to be caused by cross sensitivity between NO and CO. NO measured is in these cases below 20 ppm, i.e., less than 1% of the measurement range of 0−2700 ppm of the analyzer.

In contrast to the results with LD slag, where some NO always survived the passage through the bed of the fuel reactor when CO was zero (see Figure 18), here, NO is zero in six cases where CO is zero. In particular, it can be noted that, while some NO passed through the bed in most of the cases at fuel additions between 0.5 and 1 L$_n$/min for LD slag, incoming NO was fully reduced by ilmenite, even at the low fuel flow of 0.25 L$_n$/min.

Thus, it is clear that ilmenite is much more effective in reducing NO than LD slag.

Similar to the test with NH$_3$ and reduced oxygen carrier, it was investigated whether the reduced oxygen carrier could reduce NO. To examine whether the oxygen carrier in its partly reduced form but in the absence of fuel is able to reduce NO, the oxygen carrier was reduced before introducing NO. The procedure is shown in Figure 26. First, syngas is added to the fuel reactor, and then air addition to the air reactor is stopped, while fuel addition is allowed to proceed for another 2 min to reduce the oxygen carrier. After the stop in fuel addition, the reduced state is conserved because only inert gas is added to the air and fuel reactors. A few minutes after the
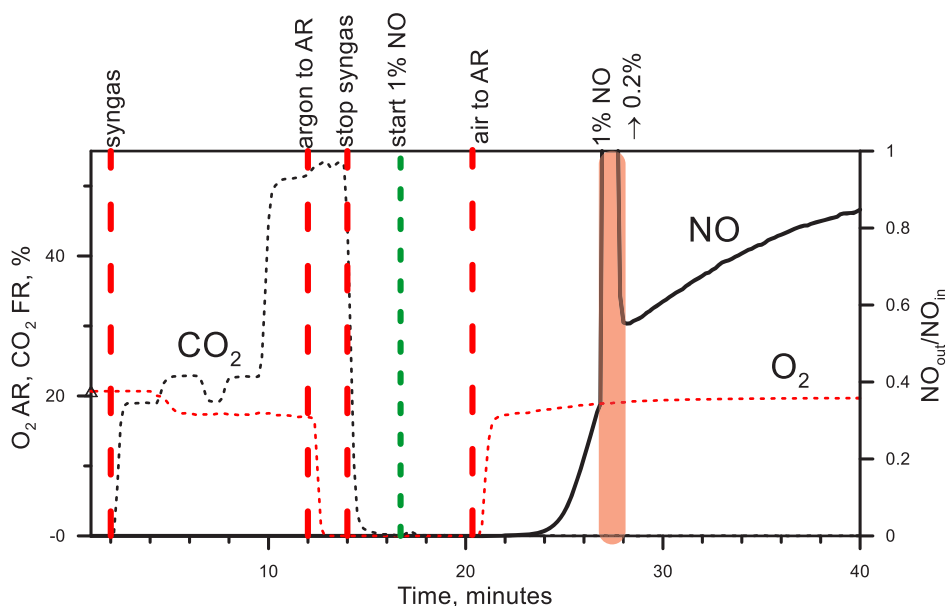
Figure 26. Ability of the reduced oxygen carrier to reduce NO in the absence of fuel.

fuel stop, the addition of NO to the fuel reactor is started. The figure clearly indicates that the reduced oxygen carrier is capable of reducing all incoming NO, even in the absence of fuel. The breakthrough of NO starts a few minutes after air addition to the air reactor has started and then slowly increases. Because the measurement range of NO is exceeded after 26−27 min, the concentration of the argon flow is switched from 1 to 0.2% NO, which creates a transient. The sharp increase is caused by starting the calculation of the NO ratio using the lower concentration, and the transient decrease needs 1−2 min to stabilize. Thus, the figure indicates that oxidation to NO only happens when ilmenite is highly oxidized.

Again, a comparison to the behavior with LD slag, which rapidly loses its ability to reduce NO in Figure 22, clearly indicates that ilmenite is much more efficient in reducing NO.

10. DISCUSSION

The most conspicuous result of the study is the fact that NO is completely reduced and that no NH_3 was oxidized to NO at any fuel flow when using ilmenite. This is in agreement with the pilot results of, i.e., Ohlemüller et al. but in disagreement with the results of Mendiara et al., Linderholm et al., and Markström et al. The latter found 1000−2000 ppm of NO (see Table 2). Most likely, this is explained by the fluidizing conditions, allowing for a significant fraction of the volatiles to bypass the bed. As pointed out in section 3, all nitrogen compounds, except N_2, are well below 1 ppm at equilibrium under the conditions in a CLC fuel reactor.

11. CONCLUSION

The oxidation of NH_3 and the breakdown of NO were studied in operation of a 300 W chemical looping reactor system, by adding either NH_3 or NO to the fluidization gas. Two different oxygen carriers, LD slag and ilmenite, were compared under varying fuel flows, temperatures, and solids circulation.

Experiments with ammonia addition and LD slag indicated the following: (1) Oxidation to NO fell with fuel flow and was essentially zero at the highest fuel flow. (2) Oxidation to NO

rose with increasing temperatures. (3) The effect of solids circulation was less clear. At the higher fuel flows, increased circulation raised conversion to NO, whereas the effect was the opposite at the lowest fuel flow. (4) In absence of CO, NO was always formed, but when conversion was incomplete, i.e., in the presence of CO, conversion to NO was always less than 1%. (5) In the absence of fuel but with the oxygen carrier partially reduced, no NO was formed.

Experiments with NO addition and LD slag indicated the following: (1) Reduction of NO increased with fuel flow. (2) Reduction of NO was higher at the low temperature. (3) Reduction of NO was higher at low circulation. (4) In the absence of CO, NO was not completely reduced, whereas in the presence of CO, NO was fully reduced. (5) In the absence of fuel but with a partly reduced oxygen carrier, NO was completely reduced.

Experiments with ammonia addition and ilmenite indicated the following: (1) In contrast to LD slag, there was no oxidation to NO at any fuel flow, even though the lowest fuel flow was half of the lowest fuel flow used for LD slag. Thus, the effect of the temperature, circulation, and fuel flow could not be assessed. (2) This also means that, in contrast to LD slag, there was no oxidation to NO for the cases when CO was zero. (3) In the absence of fuel but with the oxygen carrier partially reduced, no NO was formed. When air addition was started, it took 5 min until NO started to increase slowly. This contrasts with LD slag, where oxidation to NO started after 3 min with a rapid increase.

Experiments with NO addition and ilmenite indicated the following: (1) In contrast to LD slag, NO was completely reduced at all fuel flows, even though the lowest fuel flow was half of the lowest fuel flow used for LD slag. Thus, the effect of the temperature, circulation, and fuel flow could not be assessed. (2) This also means that, in contrast to LD slag, reduction of NO was complete also when CO was zero, i.e., in six cases. (3) In the absence of fuel but with a partly reduced oxygen carrier, NO was completely reduced. When air addition was started, it took 4 min until NO started to increase, in contrast to LD slag, where a steep increase started after 3 min.

Thus, ilmenite is much more efficient in reducing NO and much less prone to oxidize NH_3 to NO. The latter is somewhat unexpected, considering that LD slag is more efficient in oxidizing CO.

■ AUTHOR INFORMATION

Corresponding Author

Anders Lyngfelt − Division of Energy Technology, Chalmers University of Technology, 41296 Göteborg, Sweden;
○ orcid.org/0000-0002-9561-6574;
Email: anders.lyngfelt@chalmers.se

Authors

Ali Hedayati − Tecnalia, Basque Research and Technology Alliance (BRTA), 01510 Vitoria-Gasteiz, Spain

Ellen Augustsson − Halmstads Energi och Miljö AB, 30102 Halmstad, Sweden

Complete contact information is available at:
https://pubs.acs.org/10.1021/acs.energyfuels.2c00750

Notes

The authors declare no competing financial interest.

■ REFERENCES

(1) Lyngfelt, A. Chemical Looping Combustion: Status and Development Challenges. *Energy Fuels* **2020**, *34*, 9077−9093.

(2) Lyngfelt, A.; Pallarès, D.; Linderholm, C.; Lind, F.; Thunman, H.; Leckner, B. Achieving Adequate Circulation in Chemical-Looping Combustion—Design proposal for 200 MW_{th} Chemical Looping Combustion Circulating Fluidized Bed Boiler. *Energy Fuels* **2022**, DOI: 10.1021/acs.energyfuels.1c03615.

(3) Lyngfelt, A.; Mattisson, T.; Linderholm, C.; Ryden, M. Chemical-Looping Combustion of Solid Fuels—What is Needed to Reach Full-Scale? *Proceedings of the 4th International Conference on Chemical Looping*; Nanjing, China, Sept 26−28, 2016.

(4) Lyngfelt, A.; Linderholm, C. Chemical-Looping Combustion of Solid Fuels—Status and recent progress. *Energy Procedia* **2017**, *114*, 371−386.

(5) Adánez, J.; Abad, A.; Garcia-Labiano, F.; Gayán, P.; de Diego, L. Progress in Chemical-Looping Combustion and Reforming technologies. *Prog. Energy Combust. Sci.* **2012**, *38*, 215−282.

(6) Lyngfelt, A.; Brink, A.; Langørgen, Ø; Mattisson, T.; Rydén, M.; Linderholm, C. 11,000 h of Chemical-Looping Combustion Operation—Where Are We and Where Do We Want to Go? *Int. J. Greenhouse Gas Control* **2019**, *88*, 38−56.

(7) Song, T.; Shen, L. Review of reactor for chemical looping combustion of solid fuels. *Int. J. Greenhouse Gas Control* **2018**, *76*, 92−110.

(8) Abuelgasim, S.; Wang, W.; Abdalazeez, A. A brief review for chemical looping combustion as a promising CO_2 capture technology: Fundamentals and progress. *Sci. Total Environ.* **2021**, *764*, 142892.

(9) Mattisson, T.; Lyngfelt, A.; Leion, H. Chemical-looping with oxygen uncoupling for combustion of solid fuels. *Int. J. Greenhouse Gas Control* **2009**, *3*, 11−19.

(10) Lyngfelt, A.; Mattisson, T. Trestegsförbränning för Avskiljning av Koldioxid (Chemical-Looping with Oxygen Uncoupling for Separation of Carbon Dioxide). Swedish Patent Application 0500249-8, 2005.

(11) Mattisson, T.; Leion, H.; Lyngfelt, A. Chemical-looping with oxygen uncoupling using CuO/ZrO_2 with petroleum coke. *Fuel* **2009**, *88*, 683−690.

(12) Rydén, M.; Leion, H.; Mattisson, T.; Lyngfelt, A. Combined oxides as oxygen carrier material for chemical-looping with oxygen uncoupling. *Appl. Energy* **2014**, *113*, 1924−1932.

(13) Azimi, G.; Leion, H.; Mattisson, T.; Lyngfelt, A. Chemical-looping with oxygen uncoupling using combined Mn-Fe oxides, testing in batch fluidized bed. *Energy Procedia* **2011**, *4*, 370−377.

(14) Azimi, G.; Rydén, M.; Leion, H.; Mattisson, T.; Lyngfelt, A. $(Mn_yFe_{1−y})O_x$ combined oxides as oxygen carrier for chemical-looping combustion with oxygen uncoupling (CLOU). *AIChE J.* **2013**, *59*, 582−588.

(15) Hanning, M.; Frick, V.; Mattisson, T.; Rydén, M.; Lyngfelt, A. Performance of Combined Manganese−Silicon Oxygen Carriers and the Possible Effects of Adding Titania. *Energy Fuels* **2016**, *30*, 1171−1182.

(16) Källén, M.; Hallberg, P.; Rydén, M.; Mattisson, T.; Lyngfelt, A. Combined Oxides of Iron, Manganese and Silica as Oxygen Carriers for Chemical-Looping with Oxygen Uncoupling. *Fuel Process. Technol.* **2014**, *124*, 87−96.

(17) Källén, M.; Rydén, M.; Lyngfelt, A.; Mattisson, T. Chemical-looping combustion using combined iron/manganese/silicon oxygen carriers. *Appl. Energy* **2015**, *157*, 330−337.

(18) Rydén, M.; Lyngfelt, A.; Mattisson, T. Combined manganese/iron oxides as oxygen carrier for chemical looping combustion with oxygen uncoupling (CLOU) in a circulating fluidized bed reactor system. *Energy Procedia* **2011**, *4*, 341−348.

(19) Mattisson, T.; Jing, D.; Lyngfelt, A.; Rydén, M. Experimental investigation of binary and ternary combined manganese oxides for chemical-looping with oxygen uncoupling (CLOU). *Fuel* **2016**, *164*, 228−236.

(20) Abad, A.; Adánez-Rubio, I.; Gayán, P.; García-Labiano, F.; de Diego, L. F.; Adánez, J. Demonstration of chemical-looping with oxygen uncoupling (CLOU) process in a 1.5kW th continuously operating unit using a Cu-based oxygen-carrier. *Int. J. Greenhouse Gas Control* **2012**, *6*, 189−200.

(21) Adánez-Rubio, I.; Abad, A.; Gayán, P.; de Diego, L. F.; García-Labiano, F.; Adánez, J. Biomass combustion with CO_2 capture by chemical looping with oxygen uncoupling (CLOU). *Fuel Process. Technol.* **2014**, *124*, 104−114.

(22) Källén, M.; Rydén, M.; Dueso, C.; Mattisson, T.; Lyngfelt, A. $CaMn_{0.9}Mg_{0.1}O_{3−\delta}$ as Oxygen Carrier in a Gas-Fired 10 kW_{th} Chemical-Looping Combustion Unit. *Ind. Eng. Chem. Res.* **2013**, *52*, 6923−6932.

(23) Hallberg, P.; Hanning, M.; Rydén, M.; Mattisson, T.; Lyngfelt, A. Investigation of a calcium Manganite as oxygen carrier during 99 h of operation of Chemical-Looping Combustion in a 10 kW unit. *Int. J. Greenhouse Gas Control* **2016**, *53*, 222−229.

(24) Moldenhauer, P.; Hallberg, P.; Biermann, M.; Snijkers, F.; Albertsen, K.; Mattisson, T.; Lyngfelt, A. Oxygen carrier development of calcium manganite-based materials with perovskite structure for chemical looping combustion of methane. *Proceedings of the 42nd International Technical Conference on Clean Energy*; Clearwater, FL, June 11−15, 2017.

(25) Rydén, M.; Lyngfelt, A.; Mattisson, T. $CaMn_{0.875}Ti_{0.125}O_3$ as oxygen carrier for chemical-looping combustion with oxygen uncoupling (CLOU)—Experiments in continuously operating fluidized bed reactor system. *Int. J. Greenhouse Gas Control* **2011**, *5*, 356−366.

(26) Hallberg, P.; Källén, M.; Jing, D.; Snijkers, F.; van Noyen, J.; Rydén, M.; Lyngfelt, A. Experimental investigation of $CaMnO_{3−\delta}$ based oxygen carriers used in continuous Chemical-Looping Combustion. *Int. J. Chem. Eng.* **2014**, *2014*, 412517.

(27) Hallberg, P.; Rydén, M.; Mattisson, T.; Lyngfelt, A. $CaMnO_{3−\delta}$ made from low cost material examined as oxygen carrier in Chemical-Looping Combustion. *Energy Procedia* **2014**, *63*, 80−86.

(28) Schmitz, M.; Linderholm, C.; Lyngfelt, A. Chemical Looping Combustion of Sulfurous Solid Fuels using Calcium Manganite as Oxygen Carrier. *Energy Procedia* **2014**, *63*, 140−152.

(29) Schmitz, M.; Linderholm, C. Performance of calcium Manganite as oxygen carrier in chemical looping combustion of biomass in a 10 kW pilot. *Appl. Energy* **2016**, *169*, 729−737.

(30) Cabello, A.; Abad, A.; Gayán, P.; de Diego, L. F.; García-Labiano, F.; Adánez, J. Effect of operating conditions and H_2S presence on the performance of $CaMg_{0.1}Mn_{0.9}O_{3−\delta}$ perovskite material in chemical looping combustion (CLC). *Energy Fuels* **2014**, *28*, 1262−1274.

(31) Mattisson, T.; Adánez, J.; Mayer, K.; Snijkers, F.; Williams, G.; Wesker, E.; Bertsch, O.; Lyngfelt, A. Innovative Oxygen Carriers Uplifting Chemical-looping Combustion. *Energy Procedia* **2014**, *63*, 113−130.

(32) Mayer, K.; Penthor, S.; Pröll, T.; Hofbauer, H. The different demands of oxygen carriers on the reactor system of a CLC plant—Results of oxygen carrier testing in a 120 kW_{th} pilot plant. *Appl. Energy* **2015**, *157*, 323−329.

(33) Ohlemüller, P.; Reitz, M.; Ströhle, J.; Epple, B. Operation of a 1 MW_{th} chemical looping pilot plant with natural gas. *Proceedings of the IEAGHG's 7th High Temperature Solid Looping Cycles Network (HTSLCN) Meeting*; Luleå, Sweden, Sept 4−5, 2017.

(34) Ohlemüller, P.; Reitz, M.; Ströhle, J.; Epple, B. Operation of a 1 MW_{th} chemical looping pilot plant with natural gas. *Proceedings of the 9th Trondheim Conference on CO_2 Capture, Transport and Storage*; Trondheim, Norway, June 12−14, 2017.

(35) Tilland, A.; Lambert, A.; Pelletant, W.; Chiche, D.; Bounie, C.; Bertholin, S. Comparison of two oxygen carriers performances for Chemical Looping Combustion application. *Proceedings of the 9th Trondheim Conference on CO_2 Capture, Transport and Storage*; Trondheim, Norway, June 12−14, 2017.

(36) Moldenhauer, P.; Rydén, M.; Mattisson, T.; Jamal, A.; Lyngfelt, A. Chemical-Looping Combustion with Heavy Liquid Fuels in a 10 kW Pilot Plant. *Fuel Process. Technol.* **2017**, *156*, 124−137.

(37) Glarborg, P.; Jensen, A. D.; Johnsson, J. E. Fuel nitrogen conversion in solid fuel fired systems. *Prog. Energy Combust. Sci.* **2003**, *29*, 89−113.

(38) Williams, A.; Pourkashanian, M.; Jones, J.; Rowlands, L. A review of NO_x formation and reduction mechanisms in combustion systems, with particular reference to coal. *J. Inst. Energy* **1997**, *70*, 102−113.

(39) Gómez-García, M. A.; Pitchon, V.; Kiennemann, A. Pollution by nitrogen oxides: An approach to NO_x abatement using sorbing catalytic materials. *Environ. Int.* **2005**, *31*, 445−467.

(40) Johnsson, J. E. Formation and reduction of nitrogen oxides in fluidized-bed combustion. *Fuel* **1994**, *73*, 1398−1415.

(41) Hämäläinen, J. P.; Aho, M. J.; Tummavuori, J. L. Formation of nitrogen oxides from fuel-N through HCN and NH_3: A model-compound study. *Fuel* **1994**, *73*, 1894−1898.

(42) De Soete, G. G. Overall reaction rates of NO and N_2 formation from fuel nitrogen. *Symp. (Int.) Combust., [Proc.]* **1975**, *15*, 1093−1102.

(43) Miller, J. A.; Bowman, C. T. Mechanism and modeling of nitrogen chemistry in combustion. *Prog. Energy Combust. Sci.* **1989**, *15*, 287−338.

(44) Åmand, L.-E. Nitrous Oxide Emission from Circulating Fluidized Bed Combustion. Ph.D. Thesis, Chalmers University of Technology, Göteborg, Sweden, 1994.

(45) Lyngfelt, A.; Åmand, L.-E.; Leckner, B. Progress of combustion in the furnace of a circulating fluidized bed boiler. *Symp. (Int.) Combust., [Proc.]* **1996**, *26*, 3253−3259.

(46) Lyngfelt, A.; Åmand, L.-E.; Gustavsson, L.; Leckner, B. Methods for reducing the emission of nitrous oxide from fluidized bed combustion. *Energy Convers. Manage.* **1996**, *37*, 1297−1302.

(47) Lyngfelt, A.; Åmand, L.-E.; Leckner, B. Reversed air staging—A method for reduction of N_2O emissions from fluidized bed combustion of coal. *Fuel* **1998**, *77*, 953−959.

(48) Åmand, L.-E.; Leckner, B. Reduction of N_2O in a circulating fluidized-bed combustor. *Fuel* **1994**, *73*, 1389−1397.

(49) Löffler, G.; Andahazy, D.; Wartha, C.; Winter, F.; Hofbauer, H. NO_x and N_2O Formation Mechanisms—A Detailed Chemical Kinetic Modeling Study on a Single Fuel Particle in a Laboratory-Scale Fluidized Bed. *J. Energy Resour. Technol.* **2001**, *123*, 228−235.

(50) Kilpinen, P.; Kallio, S.; Konttinen, J.; Mueller, C.; Jungar, A.; Hupa, M. Towards a quantitative understanding of NO_x and N_2O emission formation in full-scale circulating fluidised bed combustors. *Proceedings of the 16th International Conference on Fluidized Bed Combustion*; Reno, NV, May 13−16, 2001.

(51) Outokumpu Research Oy. *HSC Chemistry 5.0 for Windows, Chemical Reaction and Equilibrium Software with Extensive Thermochemical Database*; Outokumpu Research Oy: Tampere, Finland, 2002.

(52) Ishida, M.; Jin, H. A novel chemical-looping combustor without NO_x formation. *Ind. Eng. Chem. Res.* **1996**, *35*, 2469−2472.

(53) Cheng, M.; Normann, F.; Zhao, D.; Li, Z.; Cai, N.; Leion, H. Oxidation of Ammonia by Ilmenite under Conditions Relevant to Chemical-Looping Combustion. *Energy Fuels* **2015**, *29*, 8126−8134.

(54) Normann, F.; Wismer, A.; Müller, C.; Leion, H. Oxidation of ammonia by iron, manganese and nickel oxides—Implications on NO_x formation in chemical-looping combustion. *Fuel* **2019**, *240*, 57−63.

(55) Normann, F.; Cheng, M.; Zhao, D.; Li, Z.; Cai, N.; Leion, H. Oxidation of Ammonia over a Copper Oxide-Containing Solid Oxygen Carrier with Oxygen Uncoupling Capability. *Combust. Flame* **2016**, *165*, 445−452.

(56) Mayrhuber, S.; Normann, F.; Yilmaz, D.; Leion, H. Effect of the Oxygen Carrier Ilmenite on NO_x Formation in Chemical-Looping Combustion. *Fuel Process. Technol.* **2021**, *222*, 106962.

(57) Song, T.; Shen, L.; Xiao, J.; Chen, D.; Gu, H.; Zhang, S. Nitrogen transfer of fuel-N in chemical looping combustion. *Combust. Flame* **2012**, *159*, 1286−1295.

(58) Song, T.; Shen, T.; Shen, L.; Xiao, J.; Gu, H.; Zhang, S. Evaluation of hematite oxygen carrier in chemical-looping combustion of coal. *Fuel* **2013**, *104*, 244−252.

(59) Markström, P.; Linderholm, C.; Lyngfelt, A. Chemical-looping combustion of solid fuels—Design and operation of a 100 kW unit with bituminous coal. *Int. J. Greenhouse Gas Control* **2013**, *15*, 150−162.

(60) Linderholm, C.; Schmitz, M.; Knutsson, P.; Källén, M.; Lyngfelt, A. Use of low-volatile fuels in a 100 kW chemical-looping combustor. *Energy Fuels* **2014**, *28*, 5942−5952.

(61) Linderholm, C.; Knutsson, P.; Schmitz, M.; Markström, P.; Lyngfelt, A. Material balances of carbon, sulfur, nitrogen and ilmenite in a 100 kW CLC reactor system. *Int. J. Greenhouse Gas Control* **2014**, *27*, 188−202.

(62) Linderholm, C.; Schmitz, M.; Knutsson, P.; Lyngfelt, A. Chemical-Looping Combustion in a 100-kW Unit using a Mixture of Ilmenite and Manganese Ore as Oxygen Carrier. *Fuel* **2016**, *166*, 533−542.

(63) Linderholm, C.; Schmitz, M. Chemical-Looping Combustion of Solid Fuels in a 100 kW Dual Circulating Fluidized Bed System using Iron Ore as Oxygen Carrier. *J. Environ. Chem. Eng.* **2016**, *4*, 1029−1039.

(64) Linderholm, C.; Schmitz, M.; Biermann, M.; Hanning, M.; Lyngfelt, A. Chemical-looping combustion of solid fuel in a 100 kW unit using sintered manganese ore as oxygen carrier. *Int. J. Greenhouse Gas Control* **2017**, *65*, 170−181.

(65) Mendiara, T.; Izquierdo, M. T.; Abad, A.; de Diego, L. F.; García-Labiano, F.; Gayán, P.; Adánez, J. Release of pollutant components in CLC of lignite. *Int. J. Greenhouse Gas Control* **2014**, *22*, 15−24.

(66) Mendiara, T.; Gayán, P.; García-Labiano, F.; de Diego, L. F.; Pérez-Astray, A.; Izquierdo, M. T.; Abad, A.; Adánez, J. Chemical looping combustion of biomass: An approach to BECCS. *Energy Procedia* **2017**, *114*, 6021−6029.

(67) Gu, H.; Shen, L.; Zhong, Z.; Niu, X.; Ge, H.; Zhou, Y.; Xiao, S.; Jiang, S. NO release during chemical looping combustion with iron ore as an oxygen carrier. *Chem. Eng. J.* **2015**, *264*, 211−220.

(68) Bayham, S. C.; Kim, H. R.; Wang, D.; Tong, A.; Zeng, L.; McGiveron, O.; Kathe, M. V.; Chung, E.; Wang, W.; Wang, A.;

Majumder, A.; Fan, L.-S. Iron-based coal direct chemical looping combustion process: 200-h continuous operation of a 25-kW$_{th}$ subpilot unit. *Energy Fuels* **2013**, *27*, 1347−1356.

(69) Ohlemüller, P.; Ströhle, J.; Epple, B. Chemical looping combustion of hard coal and torrefied biomass in a 1 MW$_{th}$ pilot plant. *Int. J. Greenhouse Gas Control* **2017**, *65*, 149−159.

(70) Hildor, F.; Mattisson, T.; Leion, H.; Linderholm, C.; Rydén, M. Steel converter slag as an oxygen carrier in a 12 MW$_{th}$ CFB boiler—Ash interaction and material evolution. *Int. J. Greenhouse Gas Control* **2019**, *88*, 321−331.

(71) Moldenhauer, P.; Linderholm, C.; Rydén, M.; Lyngfelt, A. Avoiding CO_2 capture effort and cost for negative CO_2 emissions using industrial waste in chemical-looping combustion/gasification of biomass. *Mitigation Adapt. Strategies Global Change* **2020**, *25*, 1−24.

(72) Rydén, M.; Hanning, M.; Lind, F. Oxygen Carrier Aided Combustion (OCAC) of Wood Chips in a 12 MW Circulating Fluidized Bed Boiler Using Steel Converter Slag as Bed Material. *Appl. Sci.* **2018**, *8*, 2657.

(73) Leion, H.; Lyngfelt, A.; Johansson, M.; Jerndal, E.; Mattisson, T. The use of ilmenite as an oxygen carrier in chemical-looping combustion. *Chem. Eng. Res. Des.* **2008**, *86*, 1017−1026.

(74) Azis, M. M.; Jerndal, E.; Leion, H.; Mattisson, T.; Lyngfelt, A. On the evaluation of synthetic and natural ilmenite using syngas as fuel in chemical-looping combustion (CLC). *Chem. Eng. Res. Des.* **2010**, *88*, 1505−1514.

(75) Corcoran, A.; Knutsson, P.; Thunman, H.; Lind, F. Industrial Implementation of Oxygen Carrier Aided Combustion. *Proceedings of the 5th International Conference on Chemical Looping*; Park City, UT, Sept 24−27, 2018.

(76) Lind, F.; Corcoran, A.; Andersson, B-Å; Thunman, H. 12,000 h of operation with oxygen-carriers in industrially relevant scale. *VGB PowerTech* **2017**, *7*, 82−87.

(77) Andersson, B.-Å.; Lind, F.; Corcoran, A.; Thunman, H. 4000 h of Operation with Oxygen-Carriers in Industrial Relevant Scale (75 MW$_{th}$). *Proceedings of the 4th International Conference on Chemical Looping*; Nanjing, China, Sept 26−28, 2016.

(78) Schmidt, D. Experimental testing of oxygen-carrier materials for chemical-looping combustion in a bench-scale, circulating fluidized-bed reactor. M.Sc. Thesis, Chalmers University of Technology, Gothenburg, Sweden, 2018.

(79) Johannsen, K. Experimental testing of oxygen carriers in a 300 W chemical-looping combustion reactor. M.Sc. Thesis, Chalmers University of Technology, Gothenburg, Sweden, 2018.

(80) Hedayati, A.; Soleimanisalim, A. H.; Mattisson, T.; Lyngfelt, A. Thermochemical conversion of biomass volatiles via chemical looping: Comparison of ilmenite and steel converter waste materials as oxygen carriers. *Fuel* **2022**, *313*, 122638.

(81) Moldenhauer, P.; Sundqvist, S.; Mattisson, T.; Linderholm, C. Chemical-Looping Combustion of Synthetic Biomass Volatiles with Manganese-Ore Oxygen Carriers. *Int. J. Greenhouse Gas Control* **2018**, *71*, 239−252.

(82) Markström, P.; Berguerand, N.; Lyngfelt, A. The application of a multistage-bed model for residence-time analysis in chemical-looping combustion of solid fuel. *Chem. Eng. Sci.* **2010**, *65*, 5055−5066.